



Bounded adaptive output feedback tracking control for flexible-joint robot manipulators^{*}

Hua-shan LIU[†], Yong HUANG

College of Information Science and Technology, Donghua University, Shanghai 201620, China

[†]E-mail: hs.liu@qq.com

Received Sept. 11, 2017; Revision accepted Jan. 25, 2018; Crosschecked June 11, 2018

Abstract: This paper presents a bounded adaptive output feedback tracking control approach for flexible-joint robot manipulators with parametric uncertainties and bounded torque inputs, from a systematic perspective of different (weak or strong) joint flexibilities. The singular perturbation theory and integral manifold concept are applied to decouple the dynamics of flexible-joint robot manipulators into a slow subsystem and a fast subsystem. A class of saturation functions is used to make the control law bounded, ensuring the torque control inputs are within the output limitation of the joint actuators. An adaptive control law of the projection type is adopted to handle the feed-forward term of the slow sub-controller with parametric uncertainties. Meanwhile, an approximate differential filter and a high-gain observer are utilized in the slow and fast subsystems, respectively, to estimate the unmeasurable states, making the complete closed-loop control with only position measurements of motors and links. Importantly, a corrective control scheme is proposed to break through the traditional singular perturbation approach and to make it feasible for robot manipulators with strong joint flexibility. Furthermore, an all-round and strict stability analysis of the whole control system is given. Finally, simulation results verify the superior dynamic performance of the proposed approach.

Key words: Robot manipulator; Flexible joint; Output feedback control; Bounded control; Adaptive control
<https://doi.org/10.1631/jzus.A1700485>

CLC number: TP24

1 Introduction

For flexible-joint robot manipulators, velocity measurements at joints and links are liable to be contaminated with external noise, and are frequently absent due to cost reduction of system hardware. Meanwhile, the joint actuators cannot offer the arbitrarily large torque required by the control law due to their limited power, and there always exist parametric uncertainties of the system model. However, the

majority of existing control approaches have been designed without considering all these actual conditions in one controller (Kiang et al., 2015; Nanos and Papadopoulos, 2015; Izadbakhsh, 2016; Ruderman and Iwasaki, 2016).

The output feedback tracking (OFT) control approach (Park et al., 2011; Li et al., 2013; Chen and Ge, 2015; Tong et al., 2015; Hu et al., 2018), which has aroused increasing interest in the tracking control area in recent years, provides a possible route towards making a closed-loop tracking control system for a flexible-joint robot manipulator with only position measurements. For general nonlinear systems, an adaptive neural output feedback control scheme was presented in (Chen and Ge, 2015) to deal with uncertainties and unknown external disturbances. By using the approximate output of the radial basis function neural network, the state observer and nonlinear disturbance observer are introduced to estimate

^{*} Project supported by the National Natural Science Foundation of China (No. 61203337), the Natural Science Foundation of Shanghai (No. 17ZR1400100), the Donghua University Distinguished Young Professor Program (No. B201309), and the Chen Guang Project Supported by Shanghai Municipal Education Commission and Shanghai Education Development Foundation (No. 13CG29), China
 ORCID: Hua-shan LIU, <https://orcid.org/0000-0002-8209-4922>
© Zhejiang University and Springer-Verlag GmbH Germany, part of Springer Nature 2018

unmeasurable states and unknown compound disturbances, respectively. An output feedback dynamic surface control scheme was proposed by Tong et al. (2015), where a fuzzy adaptive observer is established to estimate the unmeasurable states. For robot manipulators, Park et al. (2011) proposed an adaptive output feedback controller for electrically driven non-holonomic mobile robots with parametric uncertainties, where an adaptive observer was used to estimate the velocity signals. In (Li et al., 2013) a fuzzy adaptive output feedback controller was presented for a single-link robot manipulator with a non-rigid joint, where a fuzzy logic technique is utilized to approximate the unknown nonlinear uncertainties and to estimate the unmeasurable states.

Especially for flexible-joint robot manipulators, Yoo et al. (2008) developed an adaptive observer by using self-recurrent wavelet neural networks to estimate the velocity information of both links and joint actuators. In (Ulrich et al., 2014), a nonlinear adaptive output feedback control approach was suggested for space robot manipulators with flexible joints, where a direct adaptive control strategy was applied to stabilize the rigid manipulator dynamics, and a simple linear control law was used to improve damping of vibrations at the joints. Loria and Avila-Becerril (2014) designed a tracking controller of the proportional-derivative (PD) type plus feedforward, where the link velocity measurements were avoided by an approximate differentiation method. As an extension of Loria and Avila-Becerril (2014), Avila-Becerril et al. (2016) used approximate differentiation for link velocity measurements and a Luenberger observer for motor velocity measurements. It is noteworthy that, Loria (2016) established a theoretical foundation that the use of observers can be obviated for output-feedback tracking control.

From a review of previous studies, bounded control strategies are always necessary to handle the saturation problem of control input (Zhang and Liu, 2012, 2013; Caverly et al., 2014a, 2014b, 2016). For a two-degree-of-freedom (2DOF) manipulator with flexible links, an observer-based bounded tracking controller is proposed by Zhang and Liu (2012), where a non-linear observer of the partial-differential-equation type is designed using boundary measurements to estimate the positions and velocities of links. By the same authors, an adaptive bounded controller

is presented in (Zhang and Liu, 2013) to regulate joint position and suppress elastic vibration with compensating parametric uncertainties. For robot manipulators with flexible joints, Caverly et al. (2014a, 2014b, 2016) developed a series of bounded controllers considering modeling uncertainties. The control law presented in (Caverly et al., 2016) is composed of a bounded proportional term and a Hammerstein strictly positive real angular rate term, while the controllers in (Caverly et al., 2014a, 2014b) are of the PD type involving different saturation functions. All the proposed controllers in (Caverly et al., 2014a, 2014b, 2016) succeed in disallowing actuator saturation by guaranteeing that the applied torque is less than a specified maximum value.

Motivated by the first saturated OFT controller proposed by Loria and Nijmeijer (1998), Liu et al. (2011) presented a generalized saturated OFT approach by using singular perturbation techniques, where a class of saturation functions was invoked in the control law, and linear and nonlinear filters were optionally involved to estimate the unmeasurable states. López-Araujo et al. (2013) proposed a saturated OFT adaptive scheme for the global position stabilization of robot manipulators with bounded inputs, which imposed no saturation-avoidance restriction on the control gains. With respect to the existing saturated OFT controllers for robot manipulators, almost all the controllers are designed for robot manipulators with rigid joints and links, and few are designed for those with flexible joints.

Singularly perturbed modeling and control have been extensively studied for flexible-joint robot manipulators since they were first proved to be feasible in (Spong, 1987), due to the intuitive dynamic analysis and simple decoupling process. Its fundamental principle is decoupling the complex flexible-joint robotic model into two low-order subsystems, then designing the corresponding sub-controller and analyzing the dynamics for each subsystem. Because of the inherent limitation of such a method, the applicable precondition of it is that the joint flexibility must be weak enough, i.e. the stiffness of each flexible joint must be large enough, but in actual situations such a precondition is sometimes not satisfied. To make the singularly perturbed approach adaptable, it is possible to make flexibility compensation in the control scheme (Spong, 1987; Spong et al., 1987; Khorasani,

1992; Al-Ashoor et al., 1993; Liu et al., 2008; Yu and Chen, 2015). Spong (1987) and Spong et al. (1987) proposed a corrective controller devised to compensate for the flexibility of the system, based on the reduced flexible model, which would embody the effects of the joint flexibility, by singular perturbation theory and the concept of the integral manifold. This flexibility compensation thinking exerted an important effect on subsequent related studies (Khorasani, 1992; Al-Ashoor et al., 1993; Liu et al., 2008; Yu and Chen, 2015). It is often applied with adaptive or robust techniques for robotic systems with strong flexibility in (Khorasani, 1992; Al-Ashoor et al., 1993), especially for those free-floating space robot manipulators in (Liu et al., 2008; Yu and Chen, 2015).

The main contribution of this work is that we propose a generalized bounded adaptive OFT (BA-OFT) control approach for flexible-joint robot manipulators with parametric uncertainties and bounded torque inputs. As far as we know, this is the first time that the bounded OFT control problem has been systematically addressed in the frame of singular perturbation theory, for flexible-joint robot manipulators considering different joint flexibility. Importantly, a corrective control-based scheme is proposed to remove the restriction that the traditional singular perturbation approach only applies to robot manipulators with weak joint flexibility thus making it also applicable to those with strong joint flexibility. As a second contribution, the bound of both (slow and fast) sub-controllers and composite controllers is assured by a class of smooth saturation functions and an adaptive control law of projection type that is also used to handle the parametric uncertainties. As a third contribution, an approximate differential filter and a high gain observer are applied to achieve OFT control and to guarantee the whole closed-loop control with only position measurements of motors and links. In addition, comprehensive and strict stability analysis of both the subsystems and the whole composite control system is given.

2 Dynamics of flexible-joint manipulators

The simplified dynamics of n DOF flexible-joint robot manipulators can be written as (Spong et al., 1987; Ge, 1996):

$$\mathbf{M}(\mathbf{q})\ddot{\mathbf{q}} + \mathbf{C}(\mathbf{q}, \dot{\mathbf{q}})\dot{\mathbf{q}} + \mathbf{G}(\mathbf{q}) = \mathbf{K}(\boldsymbol{\theta} - \mathbf{q}), \quad (1)$$

$$\mathbf{J}\ddot{\boldsymbol{\theta}} + \mathbf{K}(\boldsymbol{\theta} - \mathbf{q}) = \mathbf{u}, \quad (2)$$

$$\mathbf{Z} = \mathbf{K}(\boldsymbol{\theta} - \mathbf{q}), \quad (3)$$

where $\mathbf{q} \in \mathbb{R}^n$ and $\boldsymbol{\theta} \in \mathbb{R}^n$ denote the angular displacements of the links and the motor shafts, respectively, $\mathbf{M}(\mathbf{q}) \in \mathbb{R}^{n \times n}$ is the symmetric positive-definite inertia matrix, $\mathbf{C}(\mathbf{q}, \dot{\mathbf{q}}) \in \mathbb{R}^{n \times n}$ is the centripetal-Coriolis matrix, $\mathbf{G}(\mathbf{q}) \in \mathbb{R}^n$ is the gravity vector, $\mathbf{K} \in \mathbb{R}^{n \times n}$ is a diagonal positive-definite matrix representing the joint stiffness coefficient, $\mathbf{J} \in \mathbb{R}^{n \times n}$ is the inertia matrix of the motors, $\mathbf{Z} \in \mathbb{R}^n$ is the elastic torque vector at joints, and $\mathbf{u} = [u_1, u_2, \dots, u_n]^T \in \mathbb{R}^n$ is the control input vector of the motors.

Assuming that all the stiffness coefficients k_i ($i=1, 2, \dots, n$) are of the same order of magnitude, they are written as multiples of a single large parameter k , namely,

$$\mathbf{K} = k\tilde{\mathbf{K}}, \quad (4)$$

where $\mathbf{K} = \text{diag}\{k_1, k_2, \dots, k_n\}$, $\tilde{\mathbf{K}} = \text{diag}\{\tilde{k}_1, \tilde{k}_2, \dots, \tilde{k}_n\}$.

Without loss of generality, we order $\tilde{\mathbf{K}} = \mathbf{I}$.

The following properties will be utilized in the following control design and stability analysis (Ge, 1996; Zergeroglu et al., 2000).

Property 1 $\mathbf{M}(\mathbf{q})$ is a symmetric and positive-definite inertia matrix; for an arbitrary vector $\mathbf{x} \in \mathbb{R}^n$, it satisfies the following inequality

$$m_1 \|\mathbf{x}\|^2 \leq \mathbf{x}^T \mathbf{M}(\mathbf{q}) \mathbf{x} \leq m_2 \|\mathbf{x}\|^2, \quad (5)$$

where m_1 and m_2 are known positive bounded constants, and $\|\mathbf{x}\|$ denotes the Euclidean norm of the vector \mathbf{x} .

Property 2 For an arbitrary vector $\mathbf{x} \in \mathbb{R}^n$, there exists

$$\mathbf{x}^T [\dot{\mathbf{M}}(\mathbf{q}) - 2\mathbf{C}(\mathbf{q}, \dot{\mathbf{q}})] \mathbf{x} = 0. \quad (6)$$

Property 3 Eq. (1) can be expressed in a linear parameterization form

$$\mathbf{M}(\mathbf{q})\ddot{\mathbf{q}} + \mathbf{C}(\mathbf{q}, \dot{\mathbf{q}})\dot{\mathbf{q}} + \mathbf{G}(\mathbf{q}) = \mathbf{Y}(\mathbf{q}, \dot{\mathbf{q}}, \ddot{\mathbf{q}})\mathbf{P}, \quad (7)$$

where $\mathbf{P} \in \mathbb{R}^r$ is the vector of robot parameters, $\mathbf{Y}(\mathbf{q}, \dot{\mathbf{q}}, \ddot{\mathbf{q}}) \in \mathbb{R}^{n \times r}$ is the corresponding matrix of known functions and its first two derivatives are bounded for an arbitrary vector $\mathbf{q} \in \mathbb{R}^n$. We assume that each parameter is bounded as

$$\underline{p}_i \leq p_i \leq \bar{p}_i, \quad (8)$$

where $p_i \in \mathbb{R}$ denotes the i th component of \mathbf{P} , $\underline{p}_i \in \mathbb{R}$ and $\bar{p}_i \in \mathbb{R}$ are the i th components of $\underline{\mathbf{P}} \in \mathbb{R}^r$ and $\bar{\mathbf{P}} \in \mathbb{R}^r$, respectively, which are defined as

$$\underline{\mathbf{P}} = [\underline{p}_1, \underline{p}_2, \dots, \underline{p}_r]^T, \quad \bar{\mathbf{P}} = [\bar{p}_1, \bar{p}_2, \dots, \bar{p}_r]^T. \quad (9)$$

Property 4 For any arbitrary vector $\mathbf{x} \in \mathbb{R}^n$, the time derivative of the inertia matrix and the centripetal-Coriolis matrix are upper bounded in the following manner:

$$\|\dot{\mathbf{M}}(\mathbf{x})\| \leq \zeta_m \|\dot{\mathbf{x}}\|, \quad \|\mathbf{C}(\mathbf{x}, \dot{\mathbf{x}})\| \leq \zeta_c \|\dot{\mathbf{x}}\|, \quad (10)$$

where ζ_m and ζ_c are positive constants, and $\|\mathbf{X}\|$ denotes L_2 norm of matrix \mathbf{X} .

To facilitate the expressions, we use \mathbf{M} , \mathbf{C} , and \mathbf{G} to replace $\mathbf{M}(\mathbf{q})$, $\mathbf{C}(\mathbf{q}, \dot{\mathbf{q}})$, and $\mathbf{G}(\mathbf{q})$, respectively.

3 System modeling

As the traditional singular perturbation approach can only be used in robotic systems with weak joint flexibility, in this section robot manipulators with weak flexibility and strong flexibility at joints are discussed separately. Specifically, for robot manipulators with strong joint flexibility, a corrective control law is designed and added into the controller, which makes the traditional singular perturbation approach qualified to handle plants of such a kind. For both cases, the full-order nonlinear system described by Eqs. (1)–(3) is decoupled into a slow subsystem and a fast subsystem in the form of singularly perturbed systems.

3.1 Robot manipulators with weak joint flexibility

Multiplying both sides of Eq. (1) by \mathbf{M}^{-1} and substituting Eq. (3) into it, we obtain:

$$\ddot{\mathbf{q}} = \mathbf{a}_1 \dot{\mathbf{q}} + \mathbf{a}_2 \mathbf{G} + \mathbf{A}_1 \mathbf{Z}, \quad (11)$$

where $\mathbf{a}_1 = -\mathbf{M}^{-1} \mathbf{C}$, $\mathbf{a}_2 = -\mathbf{M}^{-1}$, and $\mathbf{A}_1 = \mathbf{M}^{-1}$.

We define the perturbation parameter $\mu = 1/k$, then substitute Eqs. (2) and (11) into Eq. (3), to obtain:

$$\mu \ddot{\mathbf{Z}} = -\mathbf{a}_1 \dot{\mathbf{q}} - \mathbf{a}_2 \mathbf{G} + \mathbf{B}_2 \mathbf{u} + \mathbf{A}_2 \mathbf{Z}, \quad (12)$$

where $\mathbf{A}_2 = -\mathbf{M}^{-1} \mathbf{J}^{-1}$ and $\mathbf{B}_2 = \mathbf{J}^{-1}$.

Eqs. (11) and (12) compose the singularly perturbed model of the robot manipulators with weak joint flexibility in the traditional form, where \mathbf{q} is taken as the slow variable and \mathbf{Z} as the fast variable. The full-order model (Eqs. (11) and (12)) represents a highly complex nonlinear system that is extremely difficult to analyze or to directly design the control laws for Al-Ashoor et al. (1993).

Note that, when $\mu \rightarrow 0$, i.e. $k \rightarrow \infty$, we have $\boldsymbol{\theta} \rightarrow \mathbf{q}$, and the control torque \mathbf{u} becomes the slow control law \mathbf{u}_s and we get the slow subsystem from Eqs. (1)–(3):

$$(\mathbf{M} + \mathbf{J})\ddot{\mathbf{q}} + \mathbf{C}\dot{\mathbf{q}} + \mathbf{G} = \mathbf{u}_s. \quad (13)$$

Eq. (13) indicates the rigid part of the flexible-joint robot manipulators. It is essentially equivalent to the model of rigid robots, so the sub-controller design for the slow subsystem can refer to those methods for such robots.

Since the flexibility at joints may produce increasing oscillations, and even lead to system instability, it is non-negligible in the system modeling. Here, to describe the joint flexibility, the fast subsystem is introduced using the concept of the integral manifold.

For system Eqs. (11) and (12), an integral manifold is defined as

$$\mathbf{Z} = \mathbf{h}(\mathbf{q}, \dot{\mathbf{q}}, \mathbf{u}, \mu), \quad (14)$$

$$\dot{\mathbf{Z}} = \dot{\mathbf{h}}(\mathbf{q}, \dot{\mathbf{q}}, \mathbf{u}, \mu), \quad (15)$$

where the function $\mathbf{h}(\mathbf{q}, \dot{\mathbf{q}}, \mathbf{u}, \mu)$ is assumed to be sufficiently continuously differentiable in all of its

arguments in (Spong et al., 1987). For convenience, $\mathbf{h}(\mathbf{q}, \dot{\mathbf{q}}, \mathbf{u}, \mu)$ is written as \mathbf{h} for short.

Expanding \mathbf{u} and \mathbf{Z} in power series, respectively (Spong, 1987; Spong et al., 1987),

$$\mathbf{Z} = \mathbf{h}_0 + \mu \mathbf{h}_1 + \mu^2 \mathbf{h}_2 + \cdots + \mu^n \mathbf{h}_n + \cdots, \quad (16)$$

$$\mathbf{u} = \mathbf{u}_0 + \mu \mathbf{u}_1 + \mu^2 \mathbf{u}_2 + \cdots + \mu^n \mathbf{u}_n + \cdots, \quad (17)$$

where \mathbf{h}_0 represents the desired elastic torque, \mathbf{u}_0 indicates the slow control law, namely \mathbf{u}_s . \mathbf{u}_i and \mathbf{h}_i ($i=0, 1, \dots, n$), represent the corresponding terms of the power series expansion of \mathbf{u} and \mathbf{Z} , respectively.

Setting $\mu=0$ in Eqs. (16) and (17), and then substituting them and Eq. (14) into Eq. (12), we obtain:

$$\mu \ddot{\mathbf{h}}_0 = -\mathbf{a}_1 \dot{\mathbf{q}} - \mathbf{a}_2 \mathbf{G} + \mathbf{B}_2 \mathbf{u}_0 + \mathbf{A}_2 \mathbf{h}_0. \quad (18)$$

The elastic torque error is defined as

$$\boldsymbol{\eta} = \mathbf{h}_0 - \mathbf{Z}. \quad (19)$$

From Eqs. (12) and (18), we get the fast subsystem

$$\mu \ddot{\boldsymbol{\eta}} = -(\mathbf{J}^{-1} + \mathbf{M}^{-1}) \boldsymbol{\eta} - \mathbf{J}^{-1} \mathbf{u}_f, \quad (20)$$

where the fast control law \mathbf{u}_f is defined as

$$\mathbf{u}_f = \mu \mathbf{u}_1 + \mu^2 \mathbf{u}_2 + \cdots + \mu^n \mathbf{u}_n + \cdots. \quad (21)$$

It is typical that almost all of the previous literature (Spong, 1987; Spong et al., 1987; Khosravi and Taghirad, 2014) focus on Eq. (20) to design the fast control laws, and thus it is necessary to calculate $\boldsymbol{\eta}$ and $\ddot{\boldsymbol{\eta}}$ to obtain \mathbf{u}_f . Here we change the form of the fast system Eq. (20) by substituting Eq. (19) into it.

$$\mu \ddot{\mathbf{Z}} = -(\mathbf{J}^{-1} + \mathbf{M}^{-1}) \mathbf{Z} - \mathbf{J}^{-1} \mathbf{u}_f^*, \quad (22)$$

where \mathbf{u}_f^* represents the new fast control law based on the reshaped fast system Eq. (22) from Eq. (20), and the relationship with \mathbf{u}_f is

$$\mathbf{u}_f^* = -\mathbf{u}_f - \mu \mathbf{J} \ddot{\mathbf{h}}_0 - \mathbf{J}(\mathbf{J}^{-1} + \mathbf{M}^{-1}) \mathbf{h}_0. \quad (23)$$

Different from the commonly used model Eq. (20), the reshaped model Eq. (22) is actually a fast

subsystem with a feedforward compensation. $\boldsymbol{\eta}$ and $\ddot{\boldsymbol{\eta}}$ are not involved in the model expression, which makes the design of the fast control law more feasible in engineering realization, i.e., the design of the fast sub-controller becomes a typical tracking issue to enable \mathbf{Z} to track \mathbf{h}_0 , thus the existing tracking approaches for the rigid robot manipulators can be used here to design the fast control law.

Hence, for robot manipulators with weak joint flexibility, the dynamics is decoupled into a slow subsystem Eq. (13) and a fast subsystem Eqs. (22) and (23).

3.2 Robot manipulators with strong joint flexibility

As is known, for robot manipulators with strong joint flexibility, the traditional singular perturbation approach cannot be used directly in modeling the system. In this study, we use the integral manifold concept to design a corrective control law to artificially enhance the rigidity of the system and compensate for the deviations caused by joint flexibility.

Using the integral manifold defined by Eq. (14), the singularly perturbed model Eqs. (11) and (12) can be rewritten as

$$\ddot{\mathbf{q}} = \mathbf{a}_1 \dot{\mathbf{q}} + \mathbf{a}_2 \mathbf{G} + \mathbf{A}_1 \mathbf{h}, \quad (24)$$

$$\mu \ddot{\mathbf{h}} = -\mathbf{a}_1 \dot{\mathbf{q}} - \mathbf{a}_2 \mathbf{G} + \mathbf{B}_2 \mathbf{u} + \mathbf{A}_2 \dot{\mathbf{h}}. \quad (25)$$

Substituting Eqs. (14)–(17) into Eq. (12), we can obtain:

$$\begin{aligned} & \mu(\ddot{\mathbf{h}}_0 + \mu \ddot{\mathbf{h}}_1 + \mu^2 \ddot{\mathbf{h}}_2 + \cdots + \mu^n \ddot{\mathbf{h}}_n + \cdots) \\ &= \mathbf{A}_2(\mathbf{h}_0 + \mu \mathbf{h}_1 + \mu^2 \mathbf{h}_2 + \cdots + \mu^n \mathbf{h}_n + \cdots) - \mathbf{a}_1 \dot{\mathbf{q}} \\ & \quad - \mathbf{a}_2 \mathbf{G} + \mathbf{B}_2(\mathbf{u}_0 + \mu \mathbf{u}_1 + \mu^2 \mathbf{u}_2 + \cdots + \mu^n \mathbf{u}_n + \cdots). \end{aligned} \quad (26)$$

In respect to the same powers of μ on both sides of Eq. (26), we have

$$\mu^0 : 0 = -\mathbf{a}_1 \dot{\mathbf{q}} - \mathbf{a}_2 \mathbf{G} + \mathbf{A}_2 \mathbf{h}_0 + \mathbf{B}_2 \mathbf{u}_0, \quad (27)$$

$$\mu^1 : \ddot{\mathbf{h}}_0 = \mathbf{A}_2 \mathbf{h}_1 + \mathbf{B}_2 \mathbf{u}_1, \quad (28)$$

$$\mu^2 : \ddot{\mathbf{h}}_1 = \mathbf{A}_2 \mathbf{h}_2 + \mathbf{B}_2 \mathbf{u}_2, \quad (29)$$

and in general

$$\mu^n : \ddot{\mathbf{h}}_{n-1} = \mathbf{A}_2 \mathbf{h}_n + \mathbf{B}_2 \mathbf{u}_n. \quad (30)$$

Accordingly, from Eqs. (27)–(30), we have:

$$h_0 = A_2^{-1}(a_1\dot{q} + a_2G - B_2u_0), \quad (31)$$

$$h_1 = A_2^{-1}(\ddot{h}_0 - B_2u_1), \quad (32)$$

$$h_2 = A_2^{-1}(\ddot{h}_1 - B_2u_2), \quad (33)$$

and in general

$$h_n = A_2^{-1}(\ddot{h}_{n-1} - B_2u_n). \quad (34)$$

Noting that the perturbation parameter μ is a small constant, by neglecting the terms of high order in Eqs. (16) and (17), we have

$$Z = h_0 + \mu h_1, \quad (35)$$

$$u = u_0 + \mu u_1 \stackrel{\text{def}}{=} \bar{u}_s, \quad (36)$$

where u_1 is the corrective control law, and \bar{u}_s is the corrected slow control law.

Substituting Eqs. (31), (32), (35), and (36) into Eq. (11), we get the corrected slow subsystem:

$$\begin{aligned} \ddot{q} &= a_1\dot{q} + a_2G + A_1A_2^{-1}(a_1\dot{q} + a_2G - B_2u_0) \\ &\quad + \mu A_1A_2^{-1}(\ddot{h}_0 - B_2u_1) \\ &= (a_1 + A_1A_2^{-1}a_1)\dot{q} + (a_2 + A_1A_2^{-1}a_2)G \\ &\quad - A_1A_2^{-1}B_2u_0 + \mu A_1A_2^{-1}(\ddot{h}_0 - B_2u_1). \end{aligned} \quad (37)$$

On the other side, from Eqs. (17) and (36), the corrected fast control law can be obtained as

$$\bar{u}_f = \mu^2 u_2 + \dots + \mu^n u_n + \dots. \quad (38)$$

As for that for robot manipulators with weak joint flexibility, the corrected fast subsystem can be presented as

$$\mu \ddot{Z} = -(J^{-1} + M^{-1})Z - J^{-1}\bar{u}_f^*, \quad (39)$$

where \bar{u}_f^* is the new corrected fast control law:

$$\bar{u}_f^* = -\mu u_1 - \bar{u}_f - J\mu\ddot{h}_0 - J(J^{-1} + M^{-1})h_0. \quad (40)$$

Hence, for robot manipulators with strong joint

flexibility, the dynamics is decoupled into a slow subsystem Eq. (37) and a fast subsystem Eqs. (39) and (40).

4 Controller design

In this section, the control goal is first given, then a class of saturation functions that will be used in the bounded control is presented, and in the following part, corresponding to Section 3, taking the parametric uncertainties into consideration, bounded adaptive controllers for robot manipulators with weak flexibility and strong flexibility at joints are designed separately. Finally, an approximate differential filter and a high-gain observer are introduced to change the proposed full-state feedback controllers into OFT controllers.

4.1 Control goal

The control objective is to design a controller with bounded torque inputs and only position measurements of both motors and links, which will guarantee that the link displacements $q \in \mathbb{R}^n$ will converge asymptotically to the desired link displacements $q_d \in \mathbb{R}^n$, where q_d is assumed to be twice differentiable. q_d and its first two derivatives are bounded for all $t > 0$:

$$\|q_d\| \leq \|q_d\|_M, \quad \|\dot{q}_d\| \leq \|\dot{q}_d\|_M, \quad \|\ddot{q}_d\| \leq \|\ddot{q}_d\|_M, \quad (41)$$

where x_M denotes the maximum value of variable x .

In brief, the control goal can be expressed as

$$\forall e(0) \in \mathbb{R}^n, \quad \lim_{t \rightarrow \infty} e(t) = \mathbf{0}, \quad (42)$$

where $e(t) = q_d - q$ is the tracking error of the link position and is written as e for short.

4.2 A class of saturation functions

To make the torque inputs bounded, a class of saturation functions to be applied in the control law is defined as follows (Liu and Zhu, 2009, Liu et al., 2011):

$$\text{Sat}(x, \mathcal{A}) = [\text{sat}(x_1, \sigma_1), \text{sat}(x_2, \sigma_2), \dots, \text{sat}(x_n, \sigma_n)]^T, \quad (43)$$

where $\mathbf{x}=[x_1, x_2, \dots, x_n]^T$, $\mathbf{A}=\text{diag}\{\sigma_1, \sigma_2, \dots, \sigma_n\}$ is the saturation factor matrix used to change the approaching behaviour to the saturation bound and which can also be applied as fine-tuning parameters of the controllers, $\sigma_i \geq 1, i=1, 2, \dots, n$. In addition, we use σ_m and σ_M to represent the minimum and the maximum values of σ_i , respectively. Some useful properties of the saturation function are as follows:

(i) $\text{sat}(x_i, \sigma_i)$ is a monotone increasing function in the real domain, i.e. $\frac{\partial \text{sat}(x_i, \sigma_i)}{\partial x_i} > 0, \forall x_i \in \mathbb{R}$.

(ii) $\text{sat}(x_i, \sigma_i)x_i \geq 0$, if and only if $x_i=0$ and $\text{sat}(x_i, \sigma_i)=0, \text{sat}(x_i, \sigma_i)x_i=0, \forall x_i \in \mathbb{R}$.

(iii) $|\text{sat}(x_i, \sigma_i)| \leq p, \|\text{Sat}(\mathbf{x}, \mathbf{A})\| \leq \sqrt{n}p, \forall x_i \in \mathbb{R}, \mathbf{x} \in \mathbb{R}^n$, where p is a positive constant.

(iv) $\sigma_M \|\mathbf{x}\| \geq \alpha_1 \|\text{Sat}(\mathbf{x}, \mathbf{A})\|, \forall \mathbf{x} \in \mathbb{R}^n$, where $\alpha_1 > 0$ is small enough.

(v) $\text{Sat}(\mathbf{x}, \mathbf{A})$ is continuously differentiable and satisfies $\lambda_M \left\{ \frac{\partial \text{Sat}(\mathbf{x}, \mathbf{A})}{\partial \mathbf{x}} \right\} \leq \beta, \forall \mathbf{x} \in \mathbb{R}^n$, where $\beta > 0$ is large enough, and $\lambda_M(\mathbf{X})$ stands for the largest eigenvalue of matrix \mathbf{X} .

(vi) There always exists a large enough constant $\alpha_2 > 0$, for all $\mathbf{x} \in \Theta_\eta, \sigma_m \|\mathbf{x}\| \leq \alpha_2 \|\text{Sat}(\mathbf{x}, \mathbf{A})\|$ is satisfied, where $\Theta_\eta = \{\mathbf{x} \in \mathbb{R}^n : \|\mathbf{x}\| \leq \eta\}, \eta > 0$ is arbitrarily large.

(vii) For all $\mathbf{x} \in \Theta_\eta$, there exists $\gamma_1 > 0$ small enough and $\gamma_2 > 0$ large enough to satisfy $\gamma_1 \|\text{Sat}(\mathbf{x}, \mathbf{A})\|^2 \leq$

$$\sum_{i=1}^n \sigma_i \int_0^{x_i} \text{sat}(x_i, \sigma_i) dx_i \leq \gamma_2 \|\text{Sat}(\mathbf{x}, \mathbf{A})\|^2.$$

4.3 Bounded adaptive controller for robot manipulators with weak joint flexibility

Note that unbounded robot controllers usually show severe oscillations with large torque inputs at the joints, especially when there is a non-zero tracking error at the initial moment or/and external torque disturbances. To handle this issue for flexible-joint manipulators, the saturation functions mentioned in Section 4.2 are used to make the control law bounded.

4.3.1 Slow control law

The design of the slow control law is based on the slow subsystem Eq. (13), which indicates the rigid part of the flexible-joint robot manipulators, so the

controller design can refer to the control methods for rigid robot manipulators.

Considering the problems of torque input saturation and parametric uncertainties, motivated by Liu et al. (2011), a generalized bounded adaptive slow control law is given as

$$\mathbf{u}_s = (\hat{\mathbf{M}} + \hat{\mathbf{J}})\ddot{\mathbf{q}}_d + \hat{\mathbf{C}}\dot{\mathbf{q}}_d + \hat{\mathbf{G}} + \mathbf{K}_p \text{Sat}(\mathbf{e}, \mathbf{K}_e) + \mathbf{K}_D \text{Sat}(\dot{\mathbf{e}}, \mathbf{K}_e), \quad (44)$$

where $\mathbf{K}_p = \text{diag}\{K_{p_1}, K_{p_2}, \dots, K_{p_n}\} \in \mathbb{R}^{n \times n}$ and $\mathbf{K}_D = \text{diag}\{K_{D_1}, K_{D_2}, \dots, K_{D_n}\} \in \mathbb{R}^{n \times n}$ are the diagonal matrices of proportional and derivative gains, respectively. $\mathbf{K}_e = \text{diag}\{k_{e_1}, k_{e_2}, \dots, k_{e_n}\} \in \mathbb{R}^{n \times n}$ is the saturation factor matrix of the link position error, $\mathbf{K}_{\dot{e}} = \text{diag}\{k_{\dot{e}_1}, k_{\dot{e}_2}, \dots, k_{\dot{e}_n}\} \in \mathbb{R}^{n \times n}$ is the saturation factor matrix of the link velocity error, and $K_{p_i}, K_{D_i} > 0, k_{e_i}, k_{\dot{e}_i} \geq 1, i=1, 2, \dots, n$. $\hat{\mathbf{M}}, \hat{\mathbf{C}}, \hat{\mathbf{G}}$, and $\hat{\mathbf{J}}$ indicate the estimated values of $\mathbf{M}, \mathbf{C}, \mathbf{G}$, and \mathbf{J} , respectively.

Defining $\tilde{\mathbf{P}} = \mathbf{P} - \hat{\mathbf{P}}$, from Eq. (1) and Property 3, we can obtain:

$$\mathbf{M}\ddot{\mathbf{q}}_d + \mathbf{C}\dot{\mathbf{q}}_d + \mathbf{G} = \mathbf{Y}_1(\mathbf{q}, \dot{\mathbf{q}}, \dot{\mathbf{q}}_d, \ddot{\mathbf{q}}_d)\mathbf{P} = \mathbf{K}(\boldsymbol{\theta}_d - \mathbf{q}_d), \quad (45)$$

$$\mathbf{M}\ddot{\mathbf{q}} + \mathbf{C}\dot{\mathbf{q}} + \mathbf{G} = \mathbf{Z} = \mathbf{Y}_2(\mathbf{q}, \dot{\mathbf{q}}, \ddot{\mathbf{q}})\mathbf{P}, \quad (46)$$

$$\hat{\mathbf{M}}\ddot{\mathbf{q}}_d + \hat{\mathbf{C}}\dot{\mathbf{q}}_d + \hat{\mathbf{G}} = \mathbf{Y}_1(\mathbf{q}, \dot{\mathbf{q}}, \dot{\mathbf{q}}_d, \ddot{\mathbf{q}}_d)\hat{\mathbf{P}}, \quad (47)$$

where $\boldsymbol{\theta}_d$ is the desired position of the motor, $\mathbf{Y}_1(\mathbf{q}, \dot{\mathbf{q}}, \dot{\mathbf{q}}_d, \ddot{\mathbf{q}}_d), \mathbf{Y}_2(\mathbf{q}, \dot{\mathbf{q}}, \ddot{\mathbf{q}}) \in \mathbb{R}^{n \times n}$ are matrices of knowns, and $\hat{\mathbf{P}}$ is the time-varying estimation of \mathbf{P} . To facilitate the expressions, \mathbf{Y}_1 and \mathbf{Y}_2 are used to replace $\mathbf{Y}_1(\mathbf{q}, \dot{\mathbf{q}}, \dot{\mathbf{q}}_d, \ddot{\mathbf{q}}_d)$ and $\mathbf{Y}_2(\mathbf{q}, \dot{\mathbf{q}}, \ddot{\mathbf{q}})$, respectively.

To estimate the unknown feed-forward term $(\hat{\mathbf{M}} + \hat{\mathbf{J}})\ddot{\mathbf{q}}_d + \hat{\mathbf{C}}\dot{\mathbf{q}}_d + \hat{\mathbf{G}}$ in Eq. (44), an adaptive control law of the projection type is given as (Hong and Yao, 2007)

$$\dot{\hat{\mathbf{P}}} = \text{proj}(\boldsymbol{\Omega}_0) = \begin{cases} \mathbf{0}, & \text{if } \hat{p}_i = \underline{p}_i \text{ and } (\boldsymbol{\Omega}_0)_i < 0, \\ \mathbf{0}, & \text{if } \hat{p}_i = \bar{p}_i \text{ and } (\boldsymbol{\Omega}_0)_i > 0, \\ \boldsymbol{\Omega}_0, & \text{otherwise,} \end{cases} \quad (48)$$

where $(\boldsymbol{\Omega}_0)_i$ and \hat{p}_i denote the i th components of $\boldsymbol{\Omega}_0$ and $\hat{\boldsymbol{P}}$, respectively, and the auxiliary term $\boldsymbol{\Omega}_0 \in \mathbb{R}^r$ is designated as

$$\boldsymbol{\Omega}_0 = (\boldsymbol{\Gamma}^{-1} \boldsymbol{Y}_1)^\top (\dot{\boldsymbol{e}} + \varepsilon \text{Sat}(\boldsymbol{e}, \boldsymbol{K}_\varepsilon)), \quad (49)$$

where $\boldsymbol{\Gamma} \in \mathbb{R}^{n \times n}$ is a constant diagonal matrix, and ε is a positive constant which represents the adaptive weighting coefficient.

By Eqs. (5), (7), and (8), and property (iii) of saturation function, the bound of the slow sub-controller is assured by satisfying

$$\sup(|u_{s_i}|) = \|\boldsymbol{Y}_i\| \|\bar{\boldsymbol{p}}_i\| + \|\boldsymbol{J}_i\|_M \|\ddot{\boldsymbol{q}}_d\|_M + \sup(K_{p_i} + K_{D_i}) p, \quad (50)$$

where \boldsymbol{Y}_i and \boldsymbol{J}_i denote the i th rows of \boldsymbol{Y}_1 and \boldsymbol{J} , respectively. u_{s_i} denotes the diagonal element in the i th row of \boldsymbol{u}_s .

4.3.2 Fast control law

Recalling Eqs. (22) and (23), we order

$$\begin{aligned} \boldsymbol{u}_f^* = & -\boldsymbol{J} \mu [\ddot{\boldsymbol{h}}_0 + \boldsymbol{k}_p \text{Sat}(\boldsymbol{\eta}, \boldsymbol{K}_\eta) + \boldsymbol{k}_v \text{Sat}(\dot{\boldsymbol{\eta}}, \boldsymbol{K}_{\dot{\eta}})] \\ & - \boldsymbol{J}(\boldsymbol{J}^{-1} + \boldsymbol{M}^{-1}) \boldsymbol{h}_0, \end{aligned} \quad (51)$$

where $\boldsymbol{k}_p \in \mathbb{R}^{n \times n}$ and $\boldsymbol{k}_v \in \mathbb{R}^{n \times n}$ are constant diagonal matrices of control gains. $\boldsymbol{K}_\eta \in \mathbb{R}^{n \times n}$ and $\boldsymbol{K}_{\dot{\eta}} \in \mathbb{R}^{n \times n}$ are constant diagonal matrices representing the saturation factors.

Substituting Eq. (51) into Eq. (23), we get the fast control law as

$$\boldsymbol{u}_f = \boldsymbol{K}_p^* \text{Sat}(\boldsymbol{\eta}, \boldsymbol{K}_\eta) + \boldsymbol{K}_D^* \text{Sat}(\dot{\boldsymbol{\eta}}, \boldsymbol{K}_{\dot{\eta}}), \quad (52)$$

where $\boldsymbol{K}_p^* = \boldsymbol{J} \mu \boldsymbol{k}_p$, $\boldsymbol{K}_D^* = \boldsymbol{J} \mu \boldsymbol{k}_v$; $K_{p_i}^*, K_{D_i}^* > 0$; $k_{\eta_i}, k_{\dot{\eta}_i} \geq 1, i=1, 2, \dots, n$.

Remark 1 Controller Eq. (51) is a combination of a feed-forward term $-\boldsymbol{J}(\boldsymbol{J}^{-1} + \boldsymbol{M}^{-1}) \boldsymbol{h}_0 - \boldsymbol{J} \mu \ddot{\boldsymbol{h}}_0$ and a PD term $-\boldsymbol{J} \mu [\boldsymbol{k}_p \text{Sat}(\boldsymbol{\eta}, \boldsymbol{K}_\eta) + \boldsymbol{k}_v \text{Sat}(\dot{\boldsymbol{\eta}}, \boldsymbol{K}_{\dot{\eta}})]$, where the feed-forward term is to track the target

elastic torque and the PD term is used to eliminate the tracking errors. As presented by Eq. (52), the fast control law is a controller in PD form and there are no $\ddot{\boldsymbol{h}}_0$ and $\ddot{\boldsymbol{\eta}}$ involved, which simplifies the implementation of the fast control law.

By property (iii), the bound of the fast control input is assured with satisfying

$$\sup(|u_{f_i}|) = \sup(K_{p_i}^* + K_{D_i}^*) p, \quad (53)$$

where u_{f_i} , $K_{p_i}^*$, and $K_{D_i}^*$ denote the diagonal element in the i th row of \boldsymbol{u}_f , \boldsymbol{K}_p^* , and \boldsymbol{K}_D^* , respectively.

According to Eqs. (50) and (53), the bounds of slow control input \boldsymbol{u}_s and fast control input \boldsymbol{u}_f are both guaranteed when applying the projection-type parameter adaptation and saturation functions, i.e. the bound of the composite control input $\boldsymbol{u} = \boldsymbol{u}_s + \boldsymbol{u}_f$ is achieved.

4.4 Bounded adaptive controller for robot manipulators with strong joint flexibility

The traditional singular perturbation approach is only applicable to robot manipulators whose joint stiffness is large enough, i.e., the flexibility of the joint is weak enough. For robot manipulators with strong joint flexibility, to make the traditional singular perturbation approach feasible, a bounded adaptive scheme with corrective control is proposed in this section.

Consider the general form of dynamics for rigid robot manipulators

$$\boldsymbol{M}_r \ddot{\boldsymbol{q}} + \boldsymbol{C}_r \dot{\boldsymbol{q}} + \boldsymbol{G}_r = \boldsymbol{u}_r, \quad (54)$$

where \boldsymbol{M}_r , \boldsymbol{C}_r , \boldsymbol{G}_r , and \boldsymbol{u}_r are equivalent to \boldsymbol{M} , \boldsymbol{C} , \boldsymbol{G} , and \boldsymbol{u} as defined in Section 2. Eq. (54) can also be rewritten as

$$\ddot{\boldsymbol{q}} = -\boldsymbol{M}_r^{-1} \boldsymbol{C}_r \dot{\boldsymbol{q}} - \boldsymbol{C}_r \boldsymbol{G}_r + \boldsymbol{M}_r^{-1} \boldsymbol{u}_r. \quad (55)$$

To compensate the joint stiffness artificially for robot manipulators with strong joint flexibility, the expression of the corrected slow subsystem Eq. (37) should be as close as possible to the form of Eq. (11). In this sense, the corrective control law is designed as Eq. (40) to eliminate the related term of μ in Eq. (37).

$$\mathbf{u}_1 = \mathbf{B}_2^{-1} \ddot{\mathbf{h}}_0 = \mathbf{J} \ddot{\mathbf{h}}_0. \quad (56)$$

Substituting Eq. (56) into Eq. (37), the corrected slow subsystem is simplified as

$$\ddot{\mathbf{q}} = (\mathbf{a}_1 + \mathbf{A}_1 \mathbf{A}_2^{-1} \mathbf{a}_1) \dot{\mathbf{q}} + (\mathbf{a}_2 + \mathbf{A}_1 \mathbf{A}_2^{-1} \mathbf{a}_2) \mathbf{G} - \mathbf{A}_1 \mathbf{A}_2^{-1} \mathbf{B}_2 \mathbf{u}_0. \quad (57)$$

From Eqs. (44) and (56), the corrected slow control law for robot manipulators with strong joint flexibility is designed as

$$\begin{aligned} \bar{\mathbf{u}}_s = \mathbf{u}_s + \mu \mathbf{u}_1 = & (\hat{\mathbf{M}} + \hat{\mathbf{J}}) \ddot{\mathbf{q}}_d + \hat{\mathbf{C}} \dot{\mathbf{q}}_d + \hat{\mathbf{G}} \\ & + \mathbf{K}_p \text{Sat}(\mathbf{e}, \mathbf{K}_e) + \mathbf{K}_D \text{Sat}(\dot{\mathbf{e}}, \mathbf{K}_e) + \mu \mathbf{J} \ddot{\mathbf{h}}_0. \end{aligned} \quad (58)$$

By Eqs. (3), (5), (7), (8), and (47) and property (iii) of the saturation function, the bound of the corrected slow controller is assured with satisfying

$$\begin{aligned} \sup(|\bar{u}_{s_i}|) = & \|\mathbf{Y}_i\| \|\bar{\mathbf{p}}_i\| + \mu \|\mathbf{J}_i\|_{\text{M}} \|\dot{\mathbf{Y}}_i\| \|\bar{\mathbf{p}}_i\| \\ & + \sup(K_{p_i} + K_{D_i}) p, \end{aligned} \quad (59)$$

where $\dot{\mathbf{Y}}_i$ denotes the i th row of $\dot{\mathbf{Y}}$, and \bar{u}_{s_i} denotes the diagonal element in the i th row of $\bar{\mathbf{u}}_s$.

Similarly, for robot manipulators with strong joint flexibility, we order

$$\begin{aligned} \bar{\mathbf{u}}_f^* = & -\mathbf{J} \mu [2\ddot{\mathbf{h}}_0 + \bar{\mathbf{k}}_p \text{Sat}(\dot{\boldsymbol{\eta}}, \bar{\mathbf{K}}_{\boldsymbol{\eta}}) + \bar{\mathbf{k}}_v \text{Sat}(\dot{\boldsymbol{\eta}}, \bar{\mathbf{K}}_{\boldsymbol{\eta}})] \\ & - \mathbf{J} (\mathbf{J}^{-1} + \mathbf{M}^{-1}) \mathbf{h}_0, \end{aligned} \quad (60)$$

where $\bar{\mathbf{k}}_p \in \mathbb{R}^{n \times n}$ and $\bar{\mathbf{k}}_v \in \mathbb{R}^{n \times n}$ are constant diagonal matrices of control gains. $\bar{\mathbf{K}}_{\boldsymbol{\eta}} \in \mathbb{R}^{n \times n}$ and $\bar{\mathbf{K}}_{\dot{\boldsymbol{\eta}}} \in \mathbb{R}^{n \times n}$ are constant diagonal matrices representing the saturation factors.

From Eqs. (40) and (60), we get the corrected fast control law as

$$\bar{\mathbf{u}}_f = \bar{\mathbf{K}}_p^* \text{Sat}(\boldsymbol{\eta}, \bar{\mathbf{K}}_{\boldsymbol{\eta}}) + \bar{\mathbf{K}}_D^* \text{Sat}(\dot{\boldsymbol{\eta}}, \bar{\mathbf{K}}_{\dot{\boldsymbol{\eta}}}), \quad (61)$$

where $\bar{\mathbf{K}}_p^* = \mathbf{J} \mu \bar{\mathbf{k}}_p$, $\bar{\mathbf{K}}_D^* = \mathbf{J} \mu \bar{\mathbf{k}}_v$; $\bar{K}_{p_i}^*, \bar{K}_{D_i}^* > 0$; $\bar{k}_{\eta_i}, \bar{k}_{\dot{\eta}_i} \geq 1, i=1, 2, \dots, n$; $\bar{K}_{p_i}^*, \bar{K}_{D_i}^*, \bar{k}_{\eta_i}$, and $\bar{k}_{\dot{\eta}_i}$ re-

spectively denote the diagonal elements in the i th row of $\bar{\mathbf{K}}_p^*, \bar{\mathbf{K}}_D^*, \bar{\mathbf{K}}_{\boldsymbol{\eta}}$, and $\bar{\mathbf{K}}_{\dot{\boldsymbol{\eta}}}$.

Correspondingly, the bound of the corrected fast control input is guaranteed by satisfying

$$\sup(|\bar{u}_{f_i}|) = \sup(\bar{K}_{p_i}^* + \bar{K}_{D_i}^*) p, \quad (62)$$

where \bar{u}_{f_i} , $\bar{K}_{p_i}^*$, and $\bar{K}_{D_i}^*$ denote the diagonal elements in the i th row of $\bar{\mathbf{u}}_f$, $\bar{\mathbf{K}}_p^*$, and $\bar{\mathbf{K}}_D^*$, respectively.

Finally, the overall control law \mathbf{u} consists of a corrected slow control law $\bar{\mathbf{u}}_s$ (with the corrective control law \mathbf{u}_1 inside) designed for the corrected slow subsystem, and a corrected fast control law $\bar{\mathbf{u}}_f$ designed for the corrected fast subsystem. Thus, the bounded composite controller for robot manipulators with strong joint flexibility is given as $\mathbf{u} = \bar{\mathbf{u}}_s + \bar{\mathbf{u}}_f = \mathbf{u}_s + \mu \mathbf{u}_1 + \bar{\mathbf{u}}_f$.

Remark 2 Importantly, the corrective control approach proposed in this study is conceived over the power series expansion of the whole composite control law \mathbf{u} , and is different from that presented in (Spong et al., 1987; Spong, 1987), which was achieved by the power series expansion of the original slow control law \mathbf{u}_s . In our work, the corrective control law \mathbf{u}_1 is proposed as a compensatory term to the original slow control law for the rigid part of a robot manipulator with strong joint flexibility. From a different point of view, since the fast control law essentially acts only on the joints, the corrective control law \mathbf{u}_1 can also be regarded as part of the original fast control law \mathbf{u}_f that is taken out to damp out the elastic oscillation at the joints, while the rest of the original fast control law is dedicated to accomplishing basic tracking control.

Remark 3 By comparing the corrective control law designed by us with the flexibility compensator proposed by Liu et al. (2008), it can be found that both of them are derived from the deformation of the original fast control law Eq. (21). The flexibility compensator is actually the proportional term of a PD controller with torque feedback, while the remaining differential term acts as the fast control law, which restricts the fast controller to a pure differential controller with respect to torque feedback, and seriously

affects its usability and flexibility. Furthermore, the controller with such a flexibility compensator as proposed by Liu et al. (2008) is unbounded.

4.5 State estimation

As is known, one of the disadvantages in formulating the dynamic model for control design purposes is that any proposed full-state feedback controller will require additional sensors for implementation. The inclusion of additional sensors to measure the velocity signals will certainly add to the cost and physical complexity of the robotic systems. Moreover, velocity measurement devices are usually contaminated with noise that cannot be easily filtered away. To solve these problems, two state estimation approaches are introduced to ensure closed-loop control with only position measurements of both motors and links, so as to achieve OFT control for flexible-joint robot manipulators. In the slow subsystem, approximate differential filters are used in the sub-controllers Eqs. (44) and (58) to estimate the velocities of links, while in the fast subsystem, a set of high-gain observers are applied in the sub-controllers Eqs. (52) and (62) to eliminate the need for measuring the velocities of both motors and links.

4.5.1 Approximate differential filter

Note that, in the slow subsystem of a robot manipulator with either weak or strong joint flexibility, only states of links are involved. In this section, an approximate differential filter is introduced to be used in the slow subsystem to generate a pseudo velocity tracking error from the position feedback of links, and to guarantee the closed-loop control of a slow subsystem without velocity measurements of links (Liu et al., 2010, 2011, 2016; Kelly et al., 1994).

The filter is given as

$$\dot{\xi} = U(\dot{e} - \xi), \tag{63}$$

which is made up of two implementable parts:

$$\dot{r} = U\xi, \tag{64}$$

$$\xi = Ue - r, \tag{65}$$

where $r \in \mathbb{R}^n$ is an auxiliary variable, and e and ξ are respectively the input and output of the approximate

differential filter. $U = \text{diag}\{\mu_1, \mu_2, \dots, \mu_n\} \in \mathbb{R}^{n \times n}$ is the filtering gain, $\mu_i > 0, i=1, 2, \dots, n$.

The asymptotically stability of the slow subsystem with approximate differential filter is analyzed in Section 5.

Remark 4 As shown, the link velocity error \dot{e} can be replaced by a pseudo signal ξ generated by an approximate differential filter, which is actually a simple linear filter that contains only the position information of links. The approximate differential filter is applied in this study in the slow subsystems of robot manipulators with either weak or strong joint flexibility to estimate the link velocities, whereas similar filters in (Kelly et al., 1994; Liu et al., 2008) are utilized in the fast subsystem to estimate the velocity signals for motors and/or links.

4.5.2 High-gain observer

As presented by Eqs. (3) and (19), the derivative of elastic torque error $\dot{\eta}$ involved in the fast control laws Eqs. (52) and (61) can be calculated through the link velocity \dot{q} and motor velocity $\dot{\theta}$, i.e. in the full-state feedback control, velocity measurements of both links and motors are necessary. Here, motivated by Khalil and Praly (2014) and Khalil and Grizzle (1996), a high-gain observer is introduced to generate pseudo signals to surrogate the link velocity error \dot{e} and motor velocity error \dot{e}_m , guaranteeing the closed-loop control of fast subsystem with only position measurements of links and motors.

Defining $e_m = \theta_d - \theta$, we have

$$\dot{e}_m = \dot{\theta}_d - \dot{\theta}. \tag{66}$$

Through Eq. (45), the desired position, velocity and acceleration signals of the motors can be expressed as

$$\theta_d = K^{-1}Y_1P + q_d, \tag{67}$$

$$\dot{\theta}_d = K^{-1}\dot{Y}_1P + \dot{q}_d, \tag{68}$$

$$\ddot{\theta}_d = K^{-1}\ddot{Y}_1P + \ddot{q}_d. \tag{69}$$

From Eqs. (3), (45), and (46), we have

$$M\ddot{e} + C\dot{e} = Y_1P - Z. \tag{70}$$

Similarly, from Eqs. (2), (3), and (70), we can obtain:

$$\mathbf{J}\ddot{\mathbf{e}}_m - \mathbf{Z} = \mathbf{J}\ddot{\boldsymbol{\theta}}_d - \mathbf{u}. \quad (71)$$

Order $\mathbf{x}_1 = [\mathbf{e}^T, \mathbf{e}_m^T]^T \in \mathbb{R}^{2n}$, $\mathbf{x}_2 = [\dot{\mathbf{e}}^T, \dot{\mathbf{e}}_m^T]^T \in \mathbb{R}^{2n}$, and $\mathbf{x} = [\mathbf{x}_1^T, \mathbf{x}_2^T]^T \in \mathbb{R}^{4n}$, from Eqs. (70) and (71), the state error equation of flexible-joint robot manipulators can be written as

$$\begin{cases} \dot{\mathbf{x}}_1 = \mathbf{x}_2, \\ \dot{\mathbf{x}}_2 = f(\mathbf{x}, \mathbf{u}) = \begin{bmatrix} \mathbf{M}^{-1}(\mathbf{Y}_1\mathbf{P} - \mathbf{Z} - \mathbf{C}\dot{\mathbf{e}}) \\ \mathbf{J}^{-1}(\mathbf{J}\ddot{\boldsymbol{\theta}}_d - \mathbf{u} + \mathbf{Z}) \end{bmatrix}. \end{cases} \quad (72)$$

To implement closed-loop control of the whole system of robot manipulators with either weak or strong joint flexibility by using only position measurements of both links and motors, a high-gain observer is introduced below to be applied in the fast subsystem as in (Khalil and Praly, 2014):

$$\begin{cases} \dot{\hat{\mathbf{x}}}_1 = \hat{\mathbf{x}}_2 + \mathbf{y}_1(\mathbf{x}_1 - \hat{\mathbf{x}}_1), \\ \dot{\hat{\mathbf{x}}}_2 = \mathbf{y}_2(\mathbf{x}_1 - \hat{\mathbf{x}}_1), \end{cases} \quad (73)$$

where $\hat{\mathbf{x}}_1$ and $\hat{\mathbf{x}}_2$ are the approximations of \mathbf{x}_1 and \mathbf{x}_2 , respectively. $\mathbf{y}_1, \mathbf{y}_2 \in \mathbb{R}^n$ denote the gains of the observer and are both positive definite diagonal constant matrices.

Subsequently, the actual velocity signals of links and motors $\dot{\mathbf{q}}$ and $\dot{\boldsymbol{\theta}}$ in the fast subsystem can be observed as

$$[\hat{\dot{\mathbf{q}}}^T, \hat{\dot{\boldsymbol{\theta}}}^T]^T = [\dot{\mathbf{q}}_d^T, \dot{\boldsymbol{\theta}}_d^T]^T - \hat{\mathbf{x}}_2, \quad (74)$$

where $\hat{\dot{\mathbf{q}}}$ and $\hat{\dot{\boldsymbol{\theta}}}$ are the approximations of $\dot{\mathbf{q}}$ and $\dot{\boldsymbol{\theta}}$, respectively.

Remark 5 By using the high-gain observer in the fast subsystem, the full-state feedback tracking control laws Eqs. (52) and (61) become OFT control laws for systems of flexible-joint robot manipulators, with only position measurements of links and motors. When the observational results of velocities of links and motors are obtained, then the estimated derivative

of elastic torque error can be calculated through Eqs. (3) and (19). Importantly, in respect to the gains of the observer, they severely impact the convergence rate of observation error. Sometimes they can be selected large enough to get good convergence, but that inevitably results in sharp oscillations of torque control input in the existing unbounded controllers. With the saturation function contained in the proposed control laws Eqs. (52) and (61), that issue is resolved.

4.6 Full expressions of the controllers

As discussed previously, in the high-gain observer, we order $\boldsymbol{\eta} = \mathbf{Z}_d - \mathbf{Z}$ in place of Eq. (19), where $\mathbf{Z}_d \in \mathbb{R}^n$ is the elastic torque vector at joints, and is equal to \mathbf{h}_0 in Eq. (19). Then from Eq. (74) we have

$$\begin{aligned} \dot{\boldsymbol{\eta}} &= \dot{\mathbf{Z}}_d - \dot{\mathbf{Z}} = \mathbf{K}(\dot{\boldsymbol{\theta}}_d - \dot{\mathbf{q}}_d) - \mathbf{K}(\dot{\boldsymbol{\theta}} - \dot{\mathbf{q}}) \\ &= \mathbf{K}(\dot{\boldsymbol{\theta}}_d - \dot{\boldsymbol{\theta}}) - \mathbf{K}(\dot{\mathbf{q}}_d - \dot{\mathbf{q}}) = \bar{\mathbf{K}}\hat{\mathbf{x}}_2, \end{aligned} \quad (75)$$

where $\bar{\mathbf{K}} = [-\mathbf{K} \quad \mathbf{K}] \in \mathbb{R}^{n \times 2n}$.

Considering state estimators, expressions of fast control laws for robot manipulators with weak and strong joint flexibilities can be updated by substituting Eq. (75) into Eqs. (52) and (61), respectively.

According to the theoretical approaches above, the full controller, including control law, adaptation law, and state estimator for a robot manipulator with weak joint flexibility can be written as

$$\begin{aligned} \mathbf{u}_s &= (\hat{\mathbf{M}} + \hat{\mathbf{J}})\ddot{\mathbf{q}}_d + \hat{\mathbf{C}}\dot{\mathbf{q}}_d + \hat{\mathbf{G}} \\ &\quad + \mathbf{K}_p\text{Sat}(\mathbf{e}, \mathbf{K}_e) + \mathbf{K}_D\text{Sat}(\boldsymbol{\xi}, \mathbf{K}_\xi), \end{aligned} \quad (76)$$

$$\mathbf{u}_f = \mathbf{K}_p^*\text{Sat}(\boldsymbol{\eta}, \mathbf{K}_\eta) + \mathbf{K}_D^*\text{Sat}(\bar{\mathbf{K}}\hat{\mathbf{x}}_2, \mathbf{K}_\eta), \quad (77)$$

where $\mathbf{K}_\xi = \text{diag}\{k_{\xi_1}, k_{\xi_2}, \dots, k_{\xi_n}\} \in \mathbb{R}^{n \times n}$ is the saturation factor matrix of the pseudo signal, and $k_{\xi_i} \geq 1$, $i=1, 2, \dots, n$.

The full controller for robot manipulators with strong joint flexibility is given as

$$\begin{aligned} \bar{\mathbf{u}}_s &= \mathbf{u}_s + \boldsymbol{\mu}\mathbf{u}_f \\ &= (\hat{\mathbf{M}} + \hat{\mathbf{J}})\ddot{\mathbf{q}}_d + \hat{\mathbf{C}}\dot{\mathbf{q}}_d + \hat{\mathbf{G}} \\ &\quad + \mathbf{K}_p\text{Sat}(\mathbf{e}, \mathbf{K}_e) + \mathbf{K}_D\text{Sat}(\boldsymbol{\xi}, \mathbf{K}_\xi) + \boldsymbol{\mu}\mathbf{J}\ddot{\mathbf{h}}_0, \end{aligned} \quad (78)$$

$$\bar{u}_f = \bar{K}_p^* \text{Sat}(\eta, \bar{K}_\eta) + \bar{K}_D^* \text{Sat}(\bar{K}_x \dot{x}_2, \bar{K}_{\dot{\eta}}). \quad (79)$$

For both controllers, the common adaptation law adopted is presented by Eqs. (48) and (49).

The block diagrams of the proposed controllers are shown in Fig. 1.

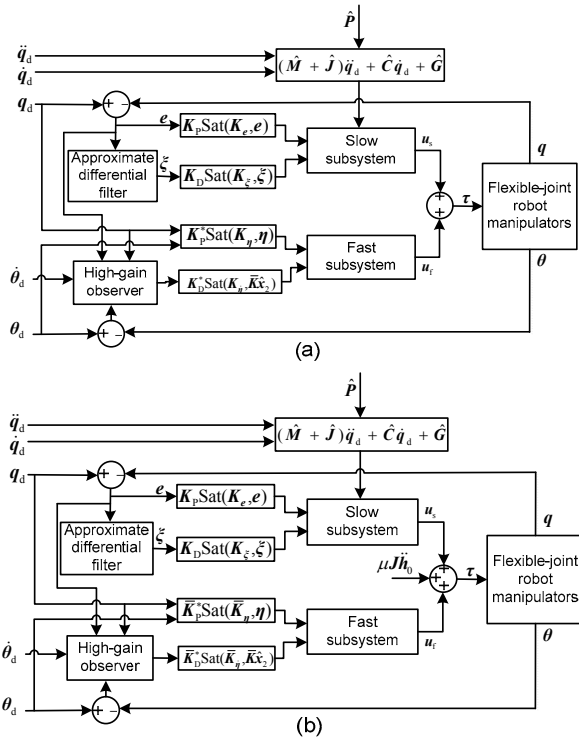


Fig. 1 Block diagrams of the controller block diagram for robot manipulators with weak joint flexibility (a) and strong joint flexibility (b)

5 Stability analysis

Considering the control systems of robot manipulators with weak joint flexibility and those with strong joint flexibility, the major difference is that the constant matrix of the joint stiffness is different, and the corrective control law u_1 for flexibility compensation (in robot manipulators with strong joint flexibility) is derived from the original fast controller u_f of the robot manipulators with weak joint flexibility. It follows that the stability analyses of the control systems of robot manipulators with weak joint flexibility and those with strong joint flexibility can both be made in the same way, and thus to avoid repetition,

only the stability proof of the former is presented in this study.

The stability of the whole control system is comprehensively analyzed by the following five steps.

Step 1: Stability analysis of the slow subsystem

Theorem 1 Considering the dynamics of the slow subsystem described by Eq. (13) with the proposed sub-controller Eq. (44), and given a desired trajectory q_d defined by Eq. (41), if the control parameters satisfy:

$$2\lambda_m(K_P) > \lambda_M(K_D),$$

and

$$\varepsilon < \min \left\{ \frac{2\gamma_1(m_1 + \lambda_m(J)) \left\{ \frac{K_{P_i}}{k_{e_i}} \right\}_m}{\sqrt{(m_2 + \lambda_M(J))^2 \left\{ \frac{K_{P_i}}{k_{e_i}} \right\}_m}}, \frac{2\alpha_1^2 \sigma_m \lambda_m(K_D)}{2\alpha_1^2 \alpha_2 \chi_E + \alpha_2 \sigma_M^2 \lambda_M(K_D)} \right\},$$

where χ_E is defined in Eq. (A12), then there is asymptotic convergence of the state and output tracking errors in the sense that $\|e\|, \|\dot{e}\| \rightarrow 0$, as $t \rightarrow \infty$.

Proof See Appendix A for details.

Step 2: Stability analysis of the fast subsystem

Theorem 2 Considering the dynamics of the fast subsystem described by Eq. (22) with the proposed sub-controller Eq. (52) in tracking control, if

$$\lambda_2 > \max \left\{ \frac{\alpha_1}{2\sigma_M}, \frac{[\sigma_M(2\lambda_1 + \lambda_2) - 4\alpha_1]^2 + \lambda_1 \alpha_1 \sigma_M}{2\lambda_1 \sigma_M^2} \right\}$$

is satisfied, then there is asymptotic convergence of the state and output tracking errors in the sense that $\|\eta\|, \|\dot{\eta}\| \rightarrow 0$, as $t \rightarrow \infty$.

Proof See Appendix B for details.

Step 3: Stability analysis of the approximate differential filters

Firstly, the stability of the approximate differential filter (that acts as the link velocity estimator in the slow subsystem) is discussed.

From Eqs. (13) and (44), the original link tracking error equation in full-state slow subsystem can be obtained as

$$(M + J)\ddot{e} + C\dot{e} = Y\tilde{P} - K_p \text{Sat}(e, K_e) - K_D \text{Sat}(\dot{e}, K_{\dot{e}}). \quad (80)$$

Considering the approximate differential filter Eq. (63), the slow subsystem with only link position measurements can be rewritten as

$$\begin{cases} (M + J)\ddot{e} + C\dot{e} = Y\tilde{P} - K_p \text{Sat}(e, K_e) - K_D \text{Sat}(\dot{e}, K_{\dot{e}}), \\ \dot{\xi} = U(\dot{e} - \xi), \end{cases} \quad (81)$$

where $K_{\xi} \in \mathbb{R}^{n \times n}$ is the saturation factor matrix of estimated velocity error.

Theorem 3 With the parameters properly selected according to $2\lambda_m(K_p) > \lambda_m(K_D)$, $8\lambda_m(K_D)\lambda_m(U^2) \geq \sigma_M^2(U^2 - K_D)$, and

$$\varepsilon < \min \left\{ \frac{\sqrt{2\gamma_1(m_1 + \lambda_m(J)) \left\{ \frac{K_{p_i}}{k_{e_i}} \right\}_m}}{\sqrt{(m_2 + \lambda_m(J))^2 \left\{ \frac{K_{p_i}}{k_{e_i}} \right\}_m}}, \frac{2\alpha_1^2 \sigma_m \lambda_m(K_D)}{2\alpha_1^2 \alpha_2 \chi_E + \alpha_2 \sigma_M^2 \lambda_m(K_D)} \right\},$$

the approximate differential filter, included in the slow subsystem, is asymptotically stable with output tracking errors $\|e\|, \|\xi\| \rightarrow 0$, as $t \rightarrow \infty$, where $\lambda_m(X)$ stands for the smallest eigenvalue of matrix X .

Proof See Appendix C for details.

Step 4: Stability analysis of the high-gain observers

Defining $\tilde{x} = [\tilde{x}_1, \tilde{x}_2]^T = [x_1 - \hat{x}_1, x_2 - \hat{x}_2]^T$ as the estimation error, from Eqs. (72) and (73), we obtain:

$$\begin{cases} \dot{\tilde{x}}_1 = -y_1 \tilde{x}_1 + \tilde{x}_2, \\ \dot{\tilde{x}}_2 = -y_2 \tilde{x}_1 + f(x, u). \end{cases} \quad (82)$$

Recalling $y_1, y_2 \in \mathbb{R}^n$ defined in Eq. (73), we order

$$y_1 = \frac{c_1}{\omega}, \quad y_2 = \frac{c_2}{\omega^2}, \quad (83)$$

where $c_1, c_2 \in \mathbb{R}^n$ are positive definite matrices, and ω is an arbitrarily small constant.

Considering the high-gain observer within the frame of singularly perturbed systems, x can be

viewed as the slow variable, and the fast variables of the observer system can be described in the time domain by using the scaled estimation error:

$$\psi_1 = \frac{\tilde{x}_1}{\omega}, \quad \psi_2 = \tilde{x}_2. \quad (84)$$

Substituting Eqs. (83) and (84) into Eq. (82), we have

$$\begin{cases} \omega \dot{\psi}_1 = -c_1 \psi_1 + \psi_2, \\ \omega \dot{\psi}_2 = -c_2 \psi_1 + \omega f(x, u). \end{cases} \quad (85)$$

At this point, the high-gain observer can be presented as Eqs. (72) and (85) in form of singularly perturbed systems.

Correspondingly, for the slow part Eq. (72), asymptotic stability is guaranteed by the converse Lyapunov theorem (Theorem 4.17) in (Khalil and Grizzle, 1996). For the fast part Eq. (85), the homogeneous expression can be written as

$$\omega \dot{\psi} = A_0 \psi, \quad (86)$$

where $A_0 = \begin{bmatrix} -c_1 & \mathbf{I} \\ -c_2 & 0 \end{bmatrix} \in \mathbb{R}^{2n \times 2n}$, $\psi = \begin{bmatrix} \psi_1 \\ \psi_2 \end{bmatrix} \in \mathbb{R}^{2n}$.

Considering a Lyapunov function candidate $W_2(\Psi) = \omega^2 \Psi^T G_0 \Psi$ for the fast part of the high-gain observer, for an arbitrarily given positive definite symmetric constant matrix Ψ_0 , there always exists a positive definite symmetric matrix G_0 as the solution of the Lyapunov equation $A_0^T G_0 + G_0 A_0 = -\Psi_0$ in Khalil and Praly (2014), i.e. W_2 is positive definite.

Differentiating V_f with respect to the fast-scaled time t/ω

$$\begin{aligned} \dot{W}_2 &= \omega \dot{\psi}^T G_0 \psi + \omega \psi^T G_0 \dot{\psi} \\ &\leq -\psi^T \lambda_m(\Psi_0) \psi \leq 0. \end{aligned} \quad (87)$$

Hence, asymptotic stability of both the slow and fast parts of the high-gain observer results in asymptotic stability of the high-gain observer included in the fast subsystem (Zhang and Liu, 2012).

Step 5: Stability analysis of the composite system

In the steps above it has been demonstrated that both the slow and fast subsystems with state

estimators are asymptotically stable. However, the stability of individual subsystems does not guarantee the stability of the composite system Eqs. (11) and (12) directly (Han and Chen, 1993; Lightcap and Banks, 2010; Khosravi and Taghirad, 2014).

Consider the following Lyapunov function candidate for the composite system

$$V = b_1 V_s + b_2 V_f, \quad (88)$$

where V_s and V_f are defined in Appendixes A and B, respectively. b_1 and b_2 are positive constants.

It can be found that V is positive definite based on the discussion above, and the time derivative of V is given by

$$\dot{V} = b_1 \dot{V}_s + b_2 \dot{V}_f. \quad (89)$$

Note that, although very similar treatments to the above steps are used here in the stability proof for the composite system, there is an important difference from Step 1 in that, Eq. (11) is used in this step to replace Eq. (13) (which appears in Step 1) to substitute into \dot{V}_s in Eq. (89), and due to that the total system is represented by Eqs. (11) and (12). The analysis related to \dot{V}_f is exactly the same as Step 2. Consequently, it is not difficult to get the negative definiteness of \dot{V} , so as to conclude that the composite system is asymptotically stable under the similar constraints in the steps above.

6 Validation example

In this part, numerical simulations are presented to verify the effectiveness of the two proposed BA-OFT controllers on a two-link robot manipulator in Ge (1996) with different joint flexibility, which is modeled by Eqs. (1)–(3).

The functions of $M(q)$, $C(q, \dot{q})$, and $G(q)$ are expressed in terms of the elements of the uncertain parameter vector $P=[p_1, p_2, p_3, p_4, p_5]^T$ as follows:

$$M(q) = \begin{bmatrix} p_1 + p_2 + 2p_3 \cos q_2 & p_2 + p_3 \cos q_2 \\ p_2 + p_3 \cos q_2 & p_2 \end{bmatrix},$$

$$C(q, \dot{q}) = \begin{bmatrix} -p_3 \dot{q}_2 \sin q_2 & -p_3 (\dot{q}_1 + \dot{q}_2) \sin q_2 \\ p_3 \dot{q}_1 \sin q_2 & 0 \end{bmatrix},$$

$$G(q) = \begin{bmatrix} (p_4 \cos q_1 + p_5 (p_1 + p_2)) g \\ p_3 g \cos (p_1 + p_2) \end{bmatrix},$$

$$J = \text{diag}\{0.1, 0.1\}, g = 9.81 \text{ m/s}^2,$$

$$\tau_{1M} = 200 \text{ Nm}, \tau_{2M} = 100 \text{ Nm},$$

where the real values of the uncertain parameters used in the simulations are set as $P=[1.66, 0.42, 0.63, 3.75, 1.25]^T$, and τ_{1M} and τ_{2M} denote the maximum output torque of the motors at the first and second joints, respectively.

Without loss of generality, the desired position trajectories for each link are given as

$$q_{d1} = q_{d2} = \frac{1}{10\pi} \sin\left(10\pi t + \frac{\pi}{6}\right) \text{ rad}.$$

6.1 Comparisons of controllers for a robot manipulator with weak joint flexibility

For a robot manipulator with weak joint flexibility, the stiffness coefficient in Eq. (4) is set as $k=10000$.

Performance comparisons are made among the proposed BA-OFT controller, the traditional adaptive controller in (Yu and Chen, 2015) with our state estimation approach (named as TA-OFT), and the traditional adaptive controller in (Yu and Chen, 2015) with our state estimation approach plus a saturation function (named as TA-OFT+SF). The proposed controller BA-OFT is expressed by Eqs. (48), (49), (63), (76), and (77), while the traditional adaptive controller in (Yu and Chen, 2015) is presented as

$$u'_s = \hat{M}\ddot{q}_r + \hat{C}\dot{q}_r + \hat{G} + K_s s, \quad (90)$$

$$\dot{P} = \Gamma^{-1} Y_1^T s, \quad (91)$$

$$u'_f = K_D^* \dot{Z}, \quad (92)$$

where $\dot{q}_r = \dot{q}_d + \Lambda e$ is the virtual reference trajectory, $s = \dot{e} + \Lambda e$ is the sliding surface, Λ is a constant matrix whose eigenvalues are strictly in the right half complex plane, K_s is a positive definite constant matrix, K_D^* is reasonably defined positive-definite diagonal

matrix, \mathbf{u}'_s and \mathbf{u}'_f denote respectively the slow control law and the fast control law in (Yu and Chen, 2015).

To make the comparisons as fair as possible, the same parameters in the controllers are selected at the same values. The saturation function $\text{sat}(\cdot)$ is selected to be $\arctan(\cdot)$ and the parameters involved are set as

$$\begin{aligned} \mathbf{K}_p &= \text{diag}\{80, 40\}, \mathbf{K}_D = \text{diag}\{40, 10\}, \\ \mathbf{K}_p^* &= \text{diag}\{30, 10\}, \mathbf{K}_D^* = \text{diag}\{10, 10\}, \\ \mathbf{U} &= \text{diag}\{500, 500\}, \mathbf{K}_D^* = \text{diag}\{0.02, 0.02\}, \\ \varepsilon &= 1.5, \mathbf{y}_1 = \text{diag}\{100, 100\}, \mathbf{y}_2 = \text{diag}\{1000, 1000\}, \\ \mathbf{K}_e &= \mathbf{K}_\xi = \text{diag}\{1, 1\}, \mathbf{K}_\eta = \mathbf{K}_\eta = \text{diag}\{0.0001, 0.0001\}, \\ \mathbf{\Gamma} &= \text{diag}\{100, 100\}, \mathbf{K}_s = \text{diag}\{80, 80\}, \mathbf{A} = \text{diag}\{10, 10\}. \end{aligned}$$

To make overall evaluation of the control performance, we adopted the following criteria (Liu et al., 2010, 2011):

Adjusting time—a period from the start to the moment when the tracking error e_i falls into the area of $\pm 10^{-3}$ rad;

Maximum torque—the maximum absolute value of τ_i from the start to the end;

RMS—root mean square of the errors, which is defined as

$$\text{RMS}(e_i) = \sqrt{\int_0^T |e_i|^2 dt / T}, \quad i = 1, 2, \quad (93)$$

$$\text{RMS}(e) = \sqrt{\int_0^T \|e\|^2 dt / T}. \quad (94)$$

Computing cycle—the average time cost of the control algorithm in a single closed-loop period.

In this study, the experimental tests were made on a laptop platform equipped with Intel(R) Celeron(R) CPU 1007U@1.50 GHz, 8 GB RAM, 64-bit Windows OS.

As shown in Fig. 2, Fig. 3, and Table 1, we find that the proposed controller BA-OFT presents the best dynamic performance, with the shortest adjusting time and the smallest RMS value of the tracking errors. Furthermore, the proposed controller has the smallest maximum torque control inputs to each joint, due to the saturation function and projection-type parameter adaptation strategy we used to make the control law bounded, which does much to suppress

the initial sharp oscillations, especially when there is non-zero tracking error of the link position at the beginning.

It is worth noting that the controller TA-OFT+SF, which greatly benefits from our state estimation approach and saturation function, shows a relatively close control performance (especially in aspects of tracking errors and control torque inputs) to the proposed controller BA-OFT, while the controller TA-OFT has a severe oscillation and fails to keep the control torque inputs within the limitation of each joint at the initial moment.

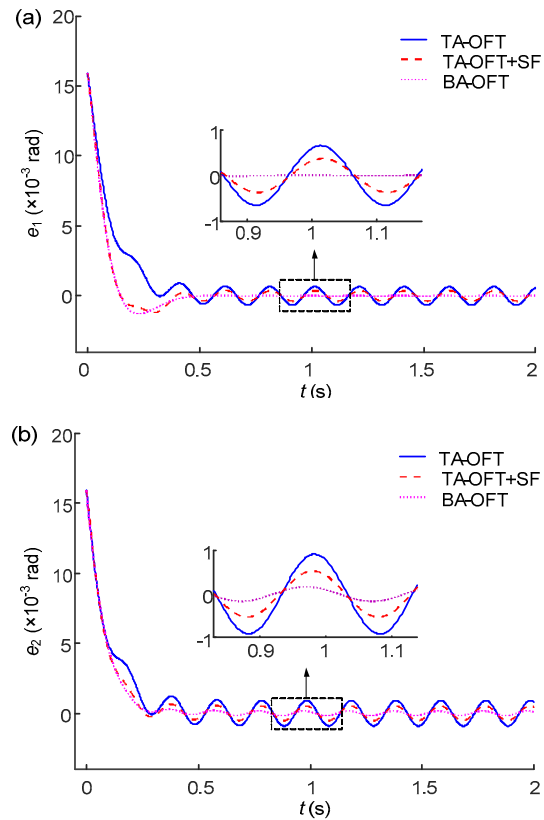


Fig. 2 Position tracking errors for link 1 (a) and link 2 (b)

6.2 Comparisons of controllers for robot manipulators with strong joint flexibility

For a robot manipulator with strong joint flexibility, numerical simulations are made on the proposed bounded adaptive OFT controller with corrective control (named as BA-OFT+CC, expressed by Eqs. (48), (49), (63), (78), and (79)), the proposed bounded adaptive OFT controller with the flexibility compensation used in (Yu and Chen, 2015) (named as

BA-OFT+FC, expressed by Eqs. (58), (61), (93), and (94)), and the traditional adaptive controller with flexibility compensation in (Yu and Chen, 2015) plus our state estimation approach (named as TA-OFT+FC, expressed by Eqs. (90), (92), (95), and (96)).

The flexibility compensated controller in (Yu and Chen, 2015) can be written as follows:

$$\mathbf{u}'_1 = \mathbf{K}_{tp} \mathbf{Z}, \tag{95}$$

$$\mathbf{u}' = \mathbf{K}_a (\mathbf{u}'_s + \mathbf{u}'_1) + \mathbf{u}'_1, \tag{96}$$

where \mathbf{u}' is the composite control law, \mathbf{u}'_1 is the flexibility compensator, and \mathbf{K}_a and \mathbf{K}_{tp} are definite positive constant matrices.

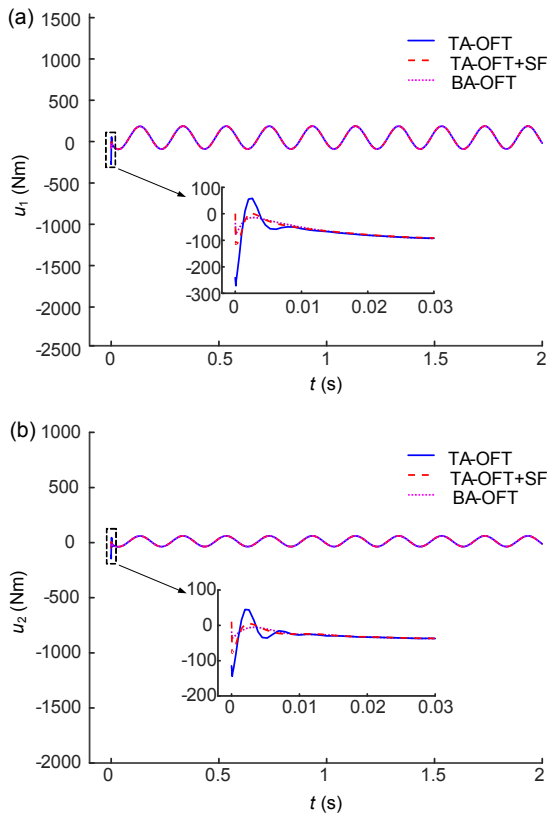


Fig. 3 Torque inputs for joint 1 (a) and joint 2 (b)

Firstly, to illustrate the effectiveness of the proposed BA-OFT+CC, we make simulations on a robot manipulator with different joint flexibilities, i.e. the joint stiffness coefficient, k , is set at 10, 50, and 100, respectively.

The parameters involved are set as follows:

$$\begin{aligned} \varepsilon &= 1.5, \mathbf{U} = \text{diag}\{1000, 1000\}, \\ \mathbf{\Gamma} &= \text{diag}\{100, 100\}, \mathbf{A} = \text{diag}\{10, 10\}, \\ \mathbf{K}_p &= \text{diag}\{100, 60\}, \mathbf{K}_D = \text{diag}\{40, 10\}, \\ \mathbf{K}_e &= \mathbf{K}_\xi = \text{diag}\{1, 1\}, \mathbf{K}_\eta = \text{diag}\{0.1, 0.1\}, \\ \mathbf{y}_1 &= \text{diag}\{100, 100\}, \mathbf{y}_2 = \text{diag}\{1000, 1000\}, \\ \bar{\mathbf{K}}_p^* &= \bar{\mathbf{K}}_D^* = \text{diag}\{10, 10\}, \mathbf{K}_\eta^* = \text{diag}\{0.001, 0.001\}, \end{aligned}$$

and the saturation function $\text{sat}(\cdot)$ is set as $\arctan(\cdot)$.

As shown in Fig. 4, the position tracking errors of both links converge quickly and are all kept in a small scale in the steady state when $k=50$ or 100, which indicates that the proposed controller BA-OFT+CC is adaptable to robot manipulators with different joint flexibilities. Specifically, when $k=10$, the robot manipulator presents an extremely strong joint flexibility, and the tracking performance is relatively worse than that when $k=50$ and 100, but the position tracking errors of both links still fall within the limit of 10^{-3} rad.

Secondly, to show the superiority of the proposed controller BA-OFT+CC, simulations are carried out comparing it to controllers BA-OFT+FC and TA-OFT+FC, where the joint stiffness coefficient is set as $k=50$, and the saturation function $\text{sat}(\cdot)$ in the control law is selected to be $\arctan(\cdot)$.

To make a fair comparison, the same parameters in the controllers are selected at the same values. The parameters involved are finally set as

$$\begin{aligned} \mathbf{\Gamma} &= \text{diag}\{100, 100\}, \mathbf{A} = \text{diag}\{10, 10\}, \\ \mathbf{K}_p &= \text{diag}\{100, 60\}, \mathbf{K}_D = \text{diag}\{40, 10\}, \\ \bar{\mathbf{K}}_p^* &= \bar{\mathbf{K}}_D^* = \text{diag}\{10, 10\}, \mathbf{K}_e = \mathbf{K}_\xi = \text{diag}\{1, 1\}, \\ \varepsilon &= 1.5, \mu = 0.02, \mathbf{K}_D^* = \text{diag}\{0.001, 0.001\}, \end{aligned}$$

Table 1 Performance comparisons in case of weak joint flexibility

Controller	Adjusting time (s)		Maximum torque (Nm)		RMS (rad)			Computing cycle (ms)
	Joint 1	Joint 2	Joint 1	Joint 2	e_1	e_2	e	
TA-OFT	0.54	0.45	271.27	143.92	0.0823	0.0804	0.1139	6.27
TA-OFT+SF	0.50	0.43	141.69	83.26	0.0795	0.0781	0.1090	9.85
BA-OFT	0.47	0.34	68.39	38.54	0.0668	0.0693	0.0967	11.32

$$\begin{aligned}
 & \mathbf{K}_s = \text{diag}\{98, 98\}, \mathbf{K}_a = \text{diag}\{5001, 5001\}, \\
 & \mathbf{K}_p = \text{diag}\{5000, 5000\}, \mathbf{U} = \text{diag}\{1000, 1000\}, \\
 & \mathbf{y}_1 = \text{diag}\{100, 100\}, \mathbf{y}_2 = \text{diag}\{1000, 1000\}.
 \end{aligned}$$

As shown in Fig. 5, Fig. 6, and Table 2, as a positive result of applying the strategies of bounded control and corrective control, the proposed controller

BA-OFT+CC presents the best control performance, with a much smaller RMS value of tracking errors and maximum torque control inputs to each joint, in comparison to the other two controllers. The unbounded controller TA-OFT+FC actually fails to restrict the torque control inputs and exceeds the limitation of the joint actuators.

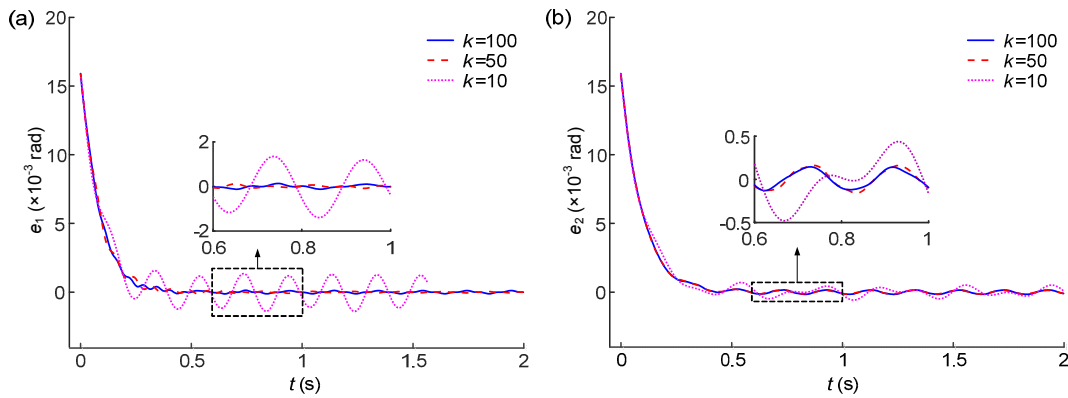


Fig. 4 Position tracking errors for link 1 (a) and link 2 (b) with different joint stiffness coefficients

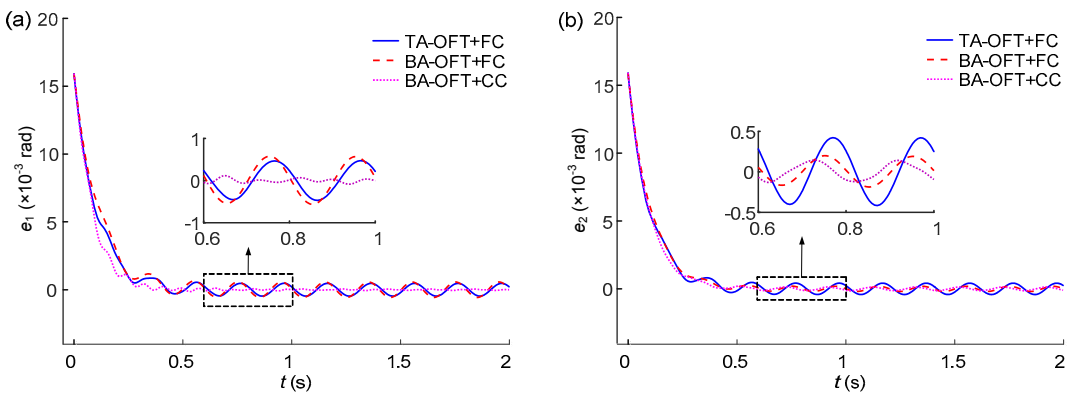


Fig. 5 Position tracking errors for link 1 (a) and link 2 (b)

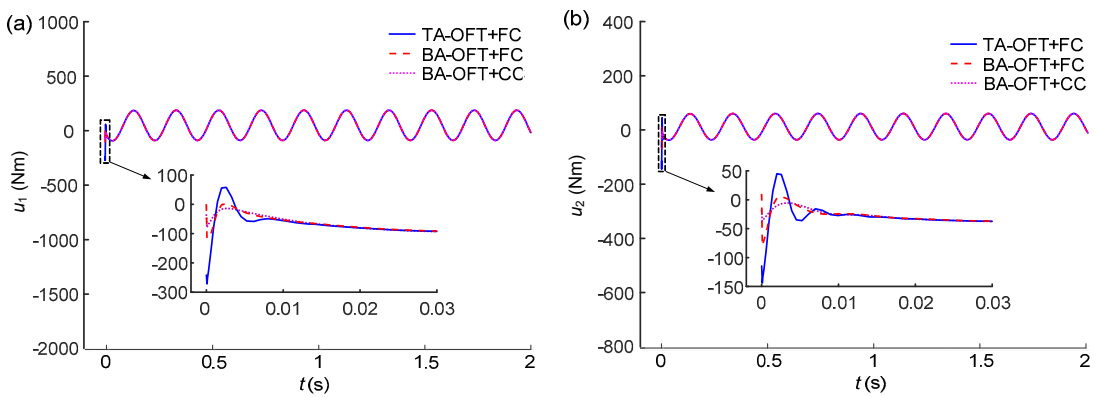


Fig. 6 Torque inputs for joint 1 (a) and joint 2 (b)

Table 2 Performance comparison in case of strong joint flexibility

Controller	Adjusting time (s)		Maximum torque (Nm)		RMS (rad)			Computing cycle (ms)
	Joint 1	Joint 2	Joint 1	Joint 2	e_1	e_2	e	
TA-OFT+FC	0.57	0.45	284.55	139.23	0.0953	0.0876	0.1308	14.56
BA-OFT+FC	0.55	0.42	133.76	92.43	0.0983	0.0689	0.1193	17.84
BA-OFT+CC	0.42	0.39	89.45	47.73	0.0096	0.0612	0.0792	19.59

7 Conclusions

This work systematically discusses BA-OFT control for robot manipulators with weak flexibility and strong flexibility at joints, in the presence of parametric uncertainties and saturated torque inputs. It is demonstrated that an adaptive control law of projection type and a general class of smooth saturation functions make the proposed controller bounded so as not to generate control torque inputs that exceed the output limitation of the joint actuators. An approximate differential filter and a high gain observer ensure the whole closed-loop control with only position measurements of motors and links. Meanwhile, the corrective control strategy helps the traditional singular perturbation approach adapt to robot manipulators with strong joint flexibility. Moreover, asymptotic stability of both subsystems and the whole composite system is achieved.

The proposed control approach is tested and evaluated on a two-link robot manipulator with parametric uncertainties. The validation results demonstrate that the proposed controllers have superior dynamic performance and the controllers using our bounded control strategy can effectively restrict the torque control inputs within the limit of the joint actuators. More importantly, the proposed BA-OFT controller with corrective control is verified as adaptable to robot manipulators with different joint flexibilities. The control approaches for robot manipulators with weak flexibility and strong flexibility at joints are shown to have high computing efficiency, that good real-time performance will be beneficial to engineering applications.

References

- Al-Ashoor RA, Patel RV, Khorasani K, 1993. Robust adaptive controller design and stability analysis for flexible-joint manipulators. *IEEE Transactions on Systems, Man, and Cybernetics*, 23(2):589-602.
<https://doi.org/10.1109/21.229473>
- Avila-Becerril S, Loría A, Panteley E, 2016. Global position-feedback tracking control of flexible-joint robots. Proceedings of the American Control Conference, p.3008-3013.
<https://doi.org/10.1109/ACC.2016.7525377>
- Caverly RJ, Zlotnik DE, Bridgeman LJ, et al., 2014a. Saturated proportional derivative control of flexible-joint manipulators. *Robotics and Computer-Integrated Manufacturing*, 30(6):658-666.
<https://doi.org/10.1016/j.rcim.2014.06.001>
- Caverly RJ, Zlotnik DE, Forbes JR, 2014b. Saturated proportional derivative control of a single-link flexible-joint manipulator. *Transactions of the Canadian Society for Mechanical Engineering*, 38(2):241-250.
- Caverly RJ, Zlotnik DE, Forbes JR, 2016. Saturated control of flexible-joint manipulators using a Hammerstein strictly positive real compensator. *Robotica*, 34(06):1367-1382.
<https://doi.org/10.1017/S0263574714002343>
- Chen M, Ge SS, 2015. Adaptive neural output feedback control of uncertain nonlinear systems with unknown hysteresis using disturbance observer. *IEEE Transactions on Industrial Electronics*, 62(12):7706-7716.
<https://doi.org/10.1109/tie.2015.2455053>
- Ge SS, 1996. Adaptive controller design for flexible joint manipulators. *Automatica*, 32(2):273-278.
[https://doi.org/10.1016/0005-1098\(96\)85559-2](https://doi.org/10.1016/0005-1098(96)85559-2)
- Han MC, Chen YH, 1993. Robust control design for uncertain flexible-joint manipulators: a singular perturbation approach. Proceedings of the 32nd IEEE Conference on Decision and Control, p.611-616.
<https://doi.org/10.1109/cdc.1993.325075>
- Hong Y, Yao B, 2007. A globally stable saturated desired compensation adaptive robust control for linear motor systems with comparative experiments. *Automatica*, 43(10):1840-1848.
<https://doi.org/10.1016/j.automatica.2007.03.021>
- Hu J, Sun X, He L, et al., 2018. Adaptive output feedback formation tracking for a class of multiagent systems with quantized input signals. *Frontiers of Information Technology & Electronic Engineering*, in press.
<https://doi.org/10.1631/FITEE.1601801>
- Izadbakhsh A, 2016. Robust control design for rigid-link flexible-joint electrically driven robot subjected to constraint: theory and experimental verification. *Nonlinear Dynamics*, 85(2):751-765.
<https://doi.org/10.1007/s11071-016-2720-6>
- Kelly R, Ortega R, Ailon A, et al., 1994. Global regulation of

- flexible joint robots using approximate differentiation. *IEEE Transactions on Automatic Control*, 39(6):1222-1224.
<https://doi.org/10.1109/9.293181>
- Khalil HK, Grizzle JW, 1996. *Nonlinear Systems*, 3rd Edition. Prentice Hall, New Jersey, USA.
- Khalil HK, Praly L, 2014. High-gain observers in nonlinear feedback control. *International Journal of Robust and Nonlinear Control*, 24(6):993-1015.
<https://doi.org/10.1002/rnc.3051>
- Khorasani K, 1992. Adaptive control of flexible-joint robots. *IEEE Transactions on Robotics and Automation*, 8(2):250-267.
<https://doi.org/10.1109/70.134278>
- Khosravi MA, Taghirad HD, 2014. Dynamic modeling and control of parallel robots with elastic cables: singular perturbation approach. *IEEE Transactions on Robotics*, 30(3):694-704.
<https://doi.org/10.1109/tro.2014.2298057>
- Kiang CT, Spowage A, Yoong CK, 2015. Review of control and sensor system of flexible manipulator. *Journal of Intelligent & Robotic Systems*, 77(1):187-213.
<https://doi.org/10.1007/s10846-014-0071-4>
- Li Y, Tong S, Li T, 2013. Adaptive fuzzy output feedback control for a single-link flexible robot manipulator driven DC motor via backstepping. *Nonlinear Analysis: Real World Applications*, 14(1):483-494.
<https://doi.org/10.1016/j.nonrwa.2012.07.010>
- Lightcap CA, Banks SA, 2010. An extended Kalman filter for real-time estimation and control of a rigid-link flexible-joint manipulator. *IEEE Transactions on Control Systems Technology*, 18(1):91-103.
<https://doi.org/10.1109/tcst.2009.2014959>
- Liu HS, Zhu SQ, 2009. A generalized trajectory tracking controller for robot manipulators with bounded inputs. *Journal of Zhejiang University-SCIENCE A*, 10(10):1500-1508.
<https://doi.org/10.1631/jzus.a0820725>
- Liu HS, Zhu SQ, Chen ZW, 2010. Saturated output feedback tracking control for robot manipulators via fuzzy self-tuning. *Journal of Zhejiang University SCIENCE C (Computers & Electronics)*, 11(12):956-966.
<https://doi.org/10.1631/jzus.c0910772>
- Liu HS, Hao KR, Lai XB, 2011. Fuzzy saturated output feedback tracking control for robot manipulators: a singular perturbation theory based approach. *International Journal of Advanced Robotic Systems*, 8(4):43-53.
<https://doi.org/10.5772/45690>
- Liu HS, Huang Y, Wu WX, 2016. Improved adaptive output feedback controller for flexible-joint robot manipulators. *Proceedings of the 2016 IEEE International Conference on Information and Automation*, p.1653-1658.
<https://doi.org/10.1109/icinf.2016.7832083>
- Liu YC, Jin MH, Liu H, 2008. Singular perturbation control for flexible-joint manipulator based on flexibility compensation. *Robot*, 30(5):460-465 (in Chinese).
<https://doi.org/10.13973/j.cnki.robot.170130>
- López-Araujo DJ, Zavala-Río A, Santibáñez V, et al., 2013. Output-feedback adaptive control for the global regulation of robot manipulators with bounded inputs. *International Journal of Control, Automation and Systems*, 11(1):105-115.
<https://doi.org/10.1007/s12555-012-9203-4>
- Loria A, 2016. Observers are unnecessary for output-feedback control of Lagrangian systems. *IEEE Transactions on Automatic Control*, 61(4):905-920.
<https://doi.org/10.1109/tac.2015.2446831>
- Loria A, Nijmeijer H, 1998. Bounded output feedback tracking control of fully actuated Euler-Lagrange systems. *Systems & Control Letters*, 33(3):151-161.
[https://doi.org/10.1016/s0167-6911\(97\)80170-3](https://doi.org/10.1016/s0167-6911(97)80170-3)
- Loria A, Avila-Becerril S, 2014. Output-feedback global tracking control of robot manipulators with flexible joints. *Proceedings of the American Control Conference*, p.4032-4037.
<https://doi.org/10.1109/acc.2014.6858900>
- Nanos K, Papadopoulos EG, 2015. On the dynamics and control of flexible joint space manipulators. *Control Engineering Practice*, 45:230-243.
<https://doi.org/10.1016/j.conengprac.2015.06.009>
- Park BS, Yoo SJ, Park JB, et al., 2011. Adaptive output-feedback control for trajectory tracking of electrically driven non-holonomic mobile robots. *IET Control Theory & Applications*, 5(6):830-838.
<https://doi.org/10.1049/iet-cta.2010.0219>
- Ruderman M, Iwasaki M, 2016. Sensorless torsion control of elastic-joint robots with hysteresis and friction. *IEEE Transactions on Industrial Electronics*, 63(3):1889-1899.
<https://doi.org/10.1109/tie.2015.2453415>
- Spong MW, 1987. Modeling and control of elastic joint robots. *Journal of Dynamic Systems, Measurement, and Control*, 109(4):310-318.
<https://doi.org/10.1115/1.3143860>
- Spong MW, Khorasani K, Kokotovic PV, 1987. An integral manifold approach to the feedback control of flexible joint robots. *IEEE Journal on Robotics and Automation*, 3(4):291-300.
<https://doi.org/10.1109/jra.1987.1087102>
- Tong S, Sui S, Li Y, 2015. Fuzzy adaptive output feedback control of MIMO nonlinear systems with partial tracking errors constrained. *IEEE Transactions on Fuzzy Systems*, 23(4):729-742.
<https://doi.org/10.1109/tfuzz.2014.2327987>
- Ulrich S, Sasiadek JZ, Barkana I, 2014. Nonlinear adaptive output feedback control of flexible-joint space manipulators with joint stiffness uncertainties. *Journal of Guidance, Control, and Dynamics*, 37(6):1961-1975.
<https://doi.org/10.2514/1.g000197>

Yoo SJ, Park JB, Choi YH, 2008. Adaptive output feedback control of flexible-joint robots using neural networks: dynamic surface design approach. *IEEE Transactions on Neural Networks*, 19(10):1712-1726.

<https://doi.org/10.1109/tnn.2008.2001266>

Yu XY, Chen L, 2015. Modeling and observer-based augmented adaptive control of flexible-joint free-floating space manipulators. *Acta Astronautica*, 108:146-155.

<https://doi.org/10.1016/j.actaastro.2014.12.002>

Zergeroglu E, Dixon W, Behal A, et al., 2000. Adaptive set-point control of robotic manipulators with amplitude-limited control inputs. *Robotica*, 18(2):171-181.

<https://doi.org/10.1017/s0263574799001988>

Zhang L, Liu J, 2012. Observer-based partial differential equation boundary control for a flexible two-link manipulator in task space. *IET Control Theory & Applications*, 6(13):2120-2133.

<https://doi.org/10.1049/iet-cta.2011.0545>

Zhang L, Liu J, 2013. Adaptive boundary control for flexible two-link manipulator based on partial differential equation dynamic model. *IET Control Theory & Applications*, 7(1):43-51.

<https://doi.org/10.1049/iet-cta.2011.0593>

Appendix A: Stability proof of the slow subsystem

Consider a Lyapunov function candidate V_s for the slow subsystem as

$$V_s = \frac{1}{2} \dot{e}^T (M + J) \dot{e} + \varepsilon \dot{e}^T (M + J) \text{Sat}(e, K_e) + \sum_{i=1}^n K_{p_i} \int_0^{e_i} \text{sat}(e_i, k_{e_i}) de_i + \frac{1}{2} \tilde{P}^T \Gamma \tilde{P}, \tag{A1}$$

where ε is the adaptive weighting coefficient defined in Eq. (49).

By Property 1 and the properties of the saturation function given in Section 4.2, we obtain:

$$V_s \geq \frac{1}{2} (m_1 + \lambda_m(J)) \|\dot{e}\|^2 - \varepsilon (m_2 + \lambda_M(J)) \|\dot{e}\| \|\text{Sat}(e, K_e)\| + \gamma_1 \left\{ \frac{K_{p_i}}{k_{e_i}} \right\}_m \|\text{Sat}(e, K_e)\|^2 + \frac{1}{2} \lambda_m(\Gamma) \|\tilde{P}\|^2. \tag{A2}$$

The Lyapunov function candidate V_s is positive definite if the following inequality is satisfied:

$$\varepsilon < \sqrt{\frac{2\gamma_1(m_1 + \lambda_m(J)) \left\{ \frac{K_{p_i}}{k_{e_i}} \right\}_m}{(m_2 + \lambda_M(J))^2}}. \tag{A3}$$

To facilitate the expressions, order $V_s = V_{s1} + V_{s2}$, where

$$V_{s1} = \dot{e}^T (M + J) \dot{e} / 2 + \varepsilon \dot{e}^T (M + J) \text{Sat}(e, K_e) + \sum_{i=1}^n K_{p_i} \int_0^{e_i} \text{sat}(e_i, k_{e_i}) de_i, V_{s2} = \frac{1}{2} \tilde{P}^T \Gamma \tilde{P}.$$

After taking the time derivatives of V_{s1} and V_{s2} , respectively, we obtain:

$$\dot{V}_{s1} = \frac{1}{2} \dot{e}^T \dot{M} \dot{e} + \dot{e}^T (M + J) \ddot{e} + \varepsilon \left[\dot{e}^T (M + J) \frac{\partial \text{Sat}(e, K_e)}{\partial e} \dot{e} + \dot{e}^T \dot{M} \text{Sat}(e, K_e) + \ddot{e}^T (M + J) \text{Sat}(e, K_e) \right] + K_p \text{Sat}(e, K_e) \dot{e}, \tag{A4}$$

$$\dot{V}_{s2} = \tilde{P}^T \Gamma \dot{\tilde{P}} = -\tilde{P}^T \Gamma \hat{P}. \tag{A5}$$

From Eqs. (13) and (44), we have

$$(M + J) \ddot{e} + C \dot{e} = \tilde{M} \ddot{q}_d + \tilde{C} \dot{q}_d + \tilde{G} - K_p \text{Sat}(e, K_e) - K_D \text{Sat}(\dot{e}, K_{\dot{e}}) = Y_1 \tilde{P} - K_p \text{Sat}(e, K_e) - K_D \text{Sat}(\dot{e}, K_{\dot{e}}). \tag{A6}$$

Then substituting Eq. (A6) into Eq. (A4), we obtain:

$$\dot{V}_{s1} = \dot{e}^T Y_1 \tilde{P} + \varepsilon \text{Sat}(e, K_e) Y_1 \tilde{P} - \dot{e}^T K_D \text{Sat}(\dot{e}, K_{\dot{e}}) + \varepsilon E - \varepsilon \text{Sat}(e, K_e) (K_p \text{Sat}(e, K_e) + K_D \text{Sat}(\dot{e}, K_{\dot{e}})), \tag{A7}$$

where

$$E = \dot{e}^T (M + J) \frac{\partial \text{Sat}(e, K_e)}{\partial e} \dot{e} + \dot{e}^T \dot{M} \text{Sat}(e, K_e) - C \dot{e} \text{Sat}(e, K_e).$$

The time derivative of V_s can be expressed as

$$\begin{aligned}\dot{V}_s &= \dot{V}_{s1} + \dot{V}_{s2} \\ &= \dot{e}^T Y_1 \tilde{P} + \varepsilon \text{Sat}(e, K_e) Y_1 \tilde{P} - \dot{e}^T K_D \text{Sat}(\dot{e}, K_e) + \varepsilon E \\ &\quad - \varepsilon \text{Sat}(e, K_e) (K_p \text{Sat}(e, K_e) + K_D \text{Sat}(\dot{e}, K_e)) \\ &\quad - \tilde{P}^T \Gamma \dot{P}.\end{aligned}\quad (\text{A8})$$

Substituting Eqs. (44), (48), and (49) into Eq. (A8), \dot{V}_s can be rewritten as

$$\begin{aligned}\dot{V}_s &= -\dot{e}^T K_D \text{Sat}(\dot{e}, K_e) + \varepsilon E \\ &\quad - \varepsilon \text{Sat}(e, K_e) (K_p \text{Sat}(e, K_e) + K_D \text{Sat}(\dot{e}, K_e)).\end{aligned}\quad (\text{A9})$$

According to property (iv) of the saturation functions, we can obtain:

$$-\dot{e}^T K_D \text{Sat}(\dot{e}, K_e) \leq -\frac{\sigma_m}{\alpha_2} \lambda_m(K_D) \|\dot{e}\|^2, \quad (\text{A10})$$

$$\begin{aligned}-\varepsilon \text{Sat}(e, K_e) K_D \text{Sat}(\dot{e}, K_e) \\ \leq \frac{1}{2} \varepsilon \lambda_M(K_D) \|\text{Sat}(e, K_e)\|^2 + \frac{1}{2} \varepsilon \frac{\sigma_M^2}{\alpha_1^2} \lambda_M(K_D) \|\dot{e}\|^2.\end{aligned}\quad (\text{A11})$$

According to Property 4, we have

$$E \leq \max\{\beta(\lambda_M(J) + m_2), \zeta_m, \zeta_c\} \|\dot{e}\|^2 \stackrel{\text{def}}{=} \chi_E \|\dot{e}\|^2. \quad (\text{A12})$$

Substituting Eqs. (A10)–(A12) into Eq. (A9), then we have

$$\begin{aligned}\dot{V}_s &\leq -\varepsilon [\lambda_m(K_p) - \lambda_M(K_D) / 2] \|\text{Sat}(e, K_e)\|^2 \\ &\quad - \left[\frac{\sigma_m}{\alpha_2} \lambda_m(K_D) - \varepsilon \left(\chi_E + \frac{\sigma_M^2}{2\alpha_1^2} \lambda_M(K_D) \right) \right] \|\dot{e}\|^2.\end{aligned}\quad (\text{A13})$$

From Eq. (A13), we can find that \dot{V}_s is negative definite if the following inequalities are satisfied:

$$2\lambda_m(K_p) > \lambda_M(K_D), \quad (\text{A14})$$

$$\varepsilon < \frac{2\alpha_1^2 \sigma_m \lambda_m(K_D)}{2\alpha_1^2 \alpha_2 \chi_E + \alpha_2 \sigma_M^2 \lambda_M(K_D)}. \quad (\text{A15})$$

Therefore, if the above conditions Eqs. (A3), (A14), and (A15) hold, the asymptotically stability of the slow subsystem is guaranteed.

Appendix B: Stability proof of the fast subsystem

Consider a Lyapunov candidate function V_f for the fast subsystem as

$$V_f = \frac{1}{2} \mu (\dot{\eta}^T \dot{\eta} + \eta^T \dot{\eta} + \eta^T \eta). \quad (\text{B1})$$

Defining $H = [\eta, \dot{\eta}]^T$, V_f can be written as

$$V_f = \frac{1}{2} \mu H^T N H \geq \frac{1}{2} \mu \lambda_m(N) \|H\|^2 \geq 0, \quad (\text{B2})$$

$$\text{where } N = \begin{bmatrix} 1 & 1/2 \\ 1/2 & 1 \end{bmatrix}.$$

Differentiating V_f with respect to the fast-scaled time $\delta = t/\mu$, and substituting Eqs. (22) and (52) into it, we then obtain:

$$\begin{aligned}\dot{V}_f &= \dot{\eta}^T \dot{\eta} + \frac{1}{2} \dot{\eta}^T \dot{\eta} + \frac{1}{2} \eta^T \ddot{\eta} + \eta^T \dot{\eta} \\ &= -\dot{\eta}^T K_p^* \text{Sat}(\eta, K_\eta) - \dot{\eta}^T K_D^* \text{Sat}(\dot{\eta}, K_{\dot{\eta}}) + \frac{1}{2} \dot{\eta}^T \dot{\eta} \\ &\quad - \frac{1}{2} \eta^T K_p^* \text{Sat}(\eta, K_\eta) - \frac{1}{2} \dot{\eta}^T K_D^* \text{Sat}(\dot{\eta}, K_{\dot{\eta}}) + \eta^T \dot{\eta}.\end{aligned}\quad (\text{B3})$$

According to property (iv) of the saturation functions, \dot{V}_f can be rewritten as

$$\begin{aligned}\dot{V}_f &\leq -\|\dot{\eta}\| \lambda_1 \frac{\sigma_M}{\alpha_1} \|\eta\| - \lambda_2 \frac{\sigma_M}{\alpha_1} \|\dot{\eta}\|^2 + \frac{1}{2} \|\dot{\eta}\|^2 \\ &\quad - \frac{1}{2} \lambda_1 \frac{\sigma_M}{\alpha_1} \|\eta\|^2 - \frac{1}{2} \|\eta\| \lambda_2 \frac{\sigma_M}{\alpha_1} \|\dot{\eta}\| + \|\eta\| \|\dot{\eta}\| \\ &\leq -T^T W T,\end{aligned}\quad (\text{B4})$$

where

$$T = \begin{bmatrix} \|\dot{\eta}\| \\ \|\eta\| \end{bmatrix},$$

$$W = \begin{bmatrix} \frac{2\lambda_2\sigma_M - \alpha_1}{2\alpha_1} & \frac{\sigma_M(2\lambda_1 + \lambda_2) - 4\alpha_1}{4\alpha_1} \\ \frac{\sigma_M(2\lambda_1 + \lambda_2) - 4\alpha_1}{4\alpha_1} & \frac{\lambda_1\sigma_M}{2\alpha_1} \end{bmatrix},$$

$$\lambda_1 = \lambda_m(K_p^*), \lambda_2 = \lambda_m(K_D^*).$$

To ensure $\dot{V}_f \leq 0$, W should be a positive definite matrix, i.e. the following inequality should be satisfied

$$\lambda_2 > \max \left\{ \frac{\alpha_1}{2\sigma_M}, \frac{[\sigma_M(2\lambda_1 + \lambda_2) - 4\alpha_1]^2 + \lambda_1\alpha_1\sigma_M}{2\lambda_1\sigma_M^2} \right\}. \tag{B5}$$

Therefore, if the above condition Eq. (B5) holds, the asymptotically stability of the fast subsystem is guaranteed.

Appendix C: Stability proof of the approximate differential filter

Consider a Lyapunov function candidate for the slow subsystem with the proposed approximate differential filter as

$$V_a = \frac{1}{2} \dot{e}^T (M + J) \dot{e} + \varepsilon \dot{e}^T (M + J) \text{Sat}(e, K_e)$$

$$+ \sum_{i=1}^n K_{p_i} \int_0^{e_i} \text{sat}(e_i, k_{e_i}) de_i + \frac{1}{2} \tilde{P}^T \Gamma \tilde{P} + \frac{1}{2} \xi^T K_D U^{-1} \xi. \tag{C1}$$

To facilitate the expressions, we partition V_a as $V_a = V_s + \xi^T K_D U^{-1} \xi / 2$, where V_s is defined by Eq. (A1).

According to Appendix A, we can find that V_a is positive definite if Eq. (A3) is satisfied.

Taking the derivative of V_a with respect to time t , we obtain:

$$\dot{V}_a = \dot{V}_s + \xi^T K_D U^{-1} \dot{\xi}$$

$$\leq \dot{V}_s - \begin{bmatrix} \|\xi\| \\ \|\dot{e}\| \end{bmatrix}^T \begin{bmatrix} \lambda_m(K_D) & \frac{\sigma_M(U^2 - K_D)}{2} \\ \frac{\sigma_M(U^2 - K_D)}{2} & 2\lambda_m(U^2) \end{bmatrix} \begin{bmatrix} \|\xi\| \\ \|\dot{e}\| \end{bmatrix}. \tag{C2}$$

According to Appendix A, if Eqs. (A14) and (A15) are satisfied, then \dot{V}_s is negative definite. Consequently, \dot{V}_a is negative definite, if the inequality (C3) is also satisfied.

$$8\lambda_m(K_D)\lambda_m(U^2) \geq \sigma_M^2(U^2 - K_D). \tag{C3}$$

Finally, the asymptotically stability of the approximate differential filter included slow subsystem can be guaranteed if the conditions Eqs. (A3), (A14), (A15), and (C3) hold.

中文概要

题目: 柔性关节机器人有界自适应输出反馈控制

目的: 考虑关节驱动力矩受限、结构参数不确定以及缺少部分传感器测量等情况, 本文研究力矩输入有界的一般柔性关节机器人自适应输出反馈控制方法, 以提高轨迹跟踪性能。

创新点: 1. 提出一种基于校正控制的强柔性关节机器人控制方法; 2. 设计一类力矩控制输入有界的自适应输出反馈轨迹跟踪控制器。

方法: 1. 引入校正控制, 突破传统奇异摄动方法仅适用于弱柔性关节机器人的限制; 2. 通过一类光滑饱和函数和投影型自适应控制律, 确保在参数不确定情况下力矩控制输入的有界性; 3. 利用近似微分滤波和高增益观测实现仅需电机侧和连杆侧位置测量的输出反馈控制。

结论: 1. 提出的校正控制策略能够较好地适应不同程度的关节柔性; 2. 设计的有界自适应输出反馈控制方法可严格确保作业全程的控制输入值有界, 且具有良好的轨迹跟踪性能。

关键词: 机器人; 柔性关节; 输出反馈控制; 有界控制; 自适应控制